Supplemental Material can be found at:
http://www.jbc.org/content/suppl/2009/08/28/M109.033431.DC1.html



NaCl fractions and dialyzed against a 20 mM Tris-HCl buffer (pH 7.6) containing 0.03% Triton X-100 and 10% glycerol.

### Assays of NADH-PQ Oxidoreductase Activity

*NADH Oxidation*—The extracts were incubated with 0.2 mM NADH in Tris-buffered saline (TBS) containing 5 μM rotenone and 1 μM *p*-hydroxymercuribenzoate at 37 °C followed by the addition of 10 mM PQ. Activities were calculated by the first-order velocity of NADH oxidation measured at $\lambda_{340\ nm}$ ($e = 6.3 \times 10^3\ M^{-1}cm^{-1}$).

*$O_2^-$ Production*—$O_2^-$ production by NADH-PQ oxidoreductase activity was assayed using a Diogenes® luminescence system (National Diagnostics Inc., Atlanta, GA). The extracts were mixed with NADH (0.1 mM), PQ (0.0012–5 mM), and Diogenes (3-fold dilution) in TBS on a 384-well plate. The effects of DIDS (100 μM) and anti-VDAC1 mAb (30 μg/ml) were evaluated by the addition of these reagents to the mixture. The total volume of the reaction mixture was 15 μl. Chemiluminescence produced by superoxide was detected by an Envision® multilabel plate reader (PerkinElmer Life Sciences).

### Immunoprecipitation

The extracts were incubated with anti-VDAC1 mAb or normal mouse IgG as a control. After incubation in TBS for 90 min at 4 °C, Protein A slurries (Amersham Biosciences) were added to the solution and gently stirred for 90 min at 4 °C. The suspensions were centrifuged, and the supernatants were obtained for the assay.

### Zymography and Western Blot Analysis

The NADH-PQ oxidoreductase fraction was mixed with 0.125 M Tris-HCl buffer (pH 6.8) containing 20% glycerol and 0.02% bromphenol blue (1:1, v/v), and the mixture was loaded on native-polyacrylamide gel (5–10% gradient gel; Funakoshi, Tokyo, Japan). Electrophoresis was performed at 5 mA for 5 h on ice, and the gel was immersed in 20 mM Tris-HCl buffer (pH 7.4) containing 20% glycerol, 0.25 mM nitro blue tetrazolium, 5 μM rotenone, and 1 μM *p*-hydroxymercuribenzoate. The gel was incubated with 2 mM NADH and 10 mM PQ at room temperature for 30 min and washed with TBS, and the active bands were stained by diformazan. The electrophoresed gel was blotted, and detection was performed with anti-VDAC1 mAb. Additionally, the active band was excised and subjected to SDS-PAGE followed by Western blot analysis with anti-VDAC1 mAb.

### Synthesis of Biotinylated PQ

The biotinylated paraquat was synthesized in moderate yield by condensation reaction of (+)-biotin and 3-(1′-methyl-4,4′-bipyridinium)propylammonium salt, which was prepared by successive *N*-alkylation of 4,4′-bipyridine with iodomethane and 3-bromopropylamine hydrobromide. See the supplemental methods for detailed procedures.

### Plasmid Construction

Human *vdac1* cDNA was isolated as an XhoI fragment by PCR and was subcloned into pUC-CAGGS expression vector (22).

### Synthesis of VDAC1 Protein Using a Cell-free Protein Synthesis System

The cDNA of VDAC1 was used. For wheat cell-free protein production of VDAC proteins, the VDAC DNA templates were constructed by "split-primer" PCR (23). The first round of PCR was performed on the cDNA using 10 nM concentrations of each of the following primers: a specific primer (5′-CCACCCACCACCACCAATGGCTGTGCCACCCACGT and AODA2306 primer, 5′-AGCGTCAGACCCCGTAGAAA). Then a second round of PCR was carried out to construct the templates for protein synthesis using a portion (5 μl) of the first PCR mix: 100 nM SPu primer (5′-GCGTAGCATTTAGGTGACACT), 100 nM AODA2303 primer (5′-GTCAGACCCCGTAGAAAAGA), and 1 nM deSP6E02 (5′-GGTGACACTATAGAACTCACCTATCTCTCTACACAAAACATTTCCCTACATACAACTTTCAACTTCCTATTCCACCCACCACCACCAATG). Wheat cell-free protein synthesis of VDAC protein was carried out using a robotic synthesizer (24, 25), GenDecorder1000® (CellFree Sciences, Yokohama, Japan) as described below. First, the transcript was created from each of the DNA templates mentioned above using SP6 RNA polymerase. The synthetic mRNAs were then precipitated with ethanol and collected by centrifugation using a Hitachi R10H rotor. Each mRNA (usually 30–35 μg) was washed and transferred into a translation mixture. The translation reaction was performed in the bilayer mode (26) with slight modifications. The translation mixture that formed the bottom layer consisted of 60 A260 units of wheat germ extract (CellFree Sciences) and 2 μg of creatine kinase (Roche Diagnostics) in 25 μl of SUB-AMIX® (CellFree Sciences). The SUB-AMIX® contained (final concentrations) 30 mM Hepes/KOH at pH 8.0, 1.2 mM ATP, 0.25 mM GTP, 16 mM creatine phosphate, 4 mM dithiothreitol, 0.4 mM spermidine, 0.3 mM concentrations of each of the 20 amino acids, 2.7 mM magnesium acetate, and 100 mM potassium acetate. 125 μl of the SUB-AMIX was placed on the top of the translation mixture, forming the upper layer. After incubation at 26 °C for 17 h, the synthesized proteins were confirmed by SDS-PAGE.

### Binding Assay

The synthesized VDAC1 protein was mixed with biotinylated PQ (0–1.0 μM) in TBS containing 10% EZ block (Atto Corp., Tokyo, Japan) for 1 h. The mixtures were added to Nunc Immobilizer® streptavidin plates (Nunc, Roskilde, Denmark), which were incubated for 2 h. The plates were then washed with TBS containing 0.1% Tween 20 (TTBS). VDAC1 protein bound to biotinylated PQ was detected by anti-VDAC1 mAb (Calbiochem) followed by the addition of horseradish peroxidase-conjugated second antibody. ECL plus® (GE Healthcare) was used as a substrate of horseradish peroxidase. For NADH binding assay, biotinylated $NAD^+$ (R&D Systems, Inc., Minneapolis, MN) was mixed with outer membrane extract, and serial dilutions of non-labeled NADH were added for 1 h. The mixtures were incubated with anti-VDAC1 mAb, which was immobilized on Nunc Immobilizer 96-well plates in 10% EZ block (Atto Corp) for 2 h. The plates were washed with TTBS to which ExtrAvidin® peroxidase (Sigma) was added followed by a wash



Downloaded from www.jbc.org at EHIME UNIVERSITY, on October 22, 2009

Supplemental Material can be found at:
http://www.jbc.org/content/suppl/2009/08/28/M109.033431.DC1.html



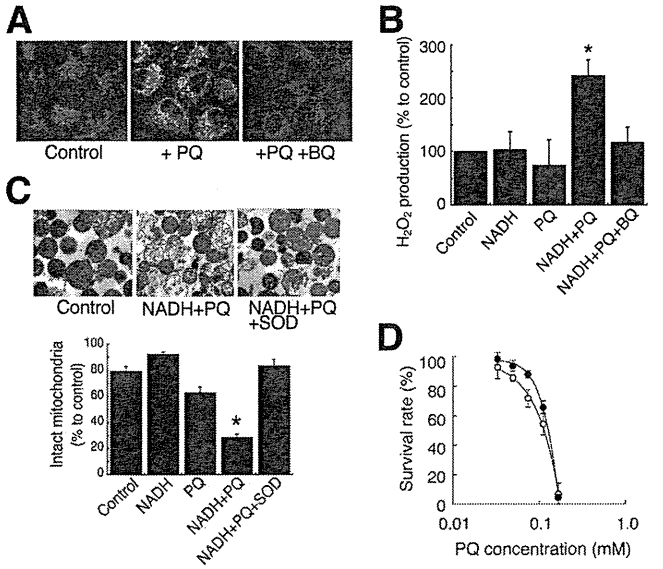


FIGURE 1. **Damage to mitochondria caused by NADH-dependent $O_2^-$ production induced by PQ.** *A*, mitochondrial $O_2^-$ production was visualized by MitoSOX in cells treated with PQ (1 mM) and BQ (0.2 mM). *B*, $H_2O_2$ production in isolated mitochondria was estimated by DCF florescence method. Mitochondria were incubated with 10 mM PQ, 2 mM NADH, and 0.3 mM BQ (*, $p <$ 0.01, *versus* control). *C*, isolated mitochondria were incubated with 3 mM PQ, 2 mM NADH, and the 3000 IU/ml SOD. *Upper panels*, electron micrograph. *Lower graph*, percentages of intact mitochondria (*, $p < 0.001$, *versus* control). *D*, the survival rate of HeLa cells exposed to PQ (*open circle*) and PQ and 1 mM Trolox® (*closed circle*). Each point is the average of two to four experiments. *Error bars* represent S.E.

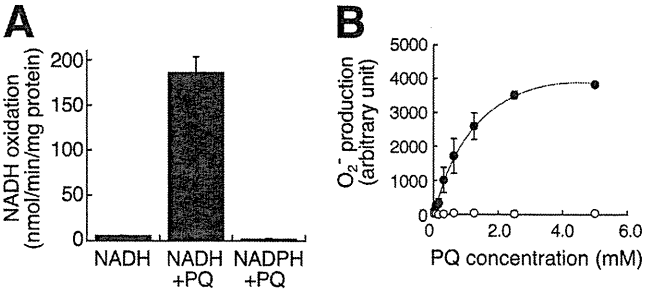


FIGURE 2. **NADH-PQ oxidoreductase activity in the outer membrane extract.** *A*, NADH (0.2 mM) was oxidized by the outer membrane extract in the presence of PQ (5 mM), but NADPH (0.2 mM) was not oxidized. *B*, PQ dose-dependent relationship to $O_2^-$ production activity was observed by co-administration with NADH (0.1 mM) to the outer membrane extract (*closed circle*). In contrast, NADPH (0.1 mM) did not exert any such PQ effects (*open circle*). All *error bars* represent S.D. ($n = 3$).

with TTBS. ECL plus was used for the detection of binding. Immobilized normal mouse IgG was used as a control.

### DNA Transfection

HeLa cells were transfected with the VDAC1 plasmid using Effectene® (Qiagen GmbH, Hilden, Germany).

### Small Interfering RNA (siRNA) Transfection

HeLa cells were transfected for 72 h with 5 nM control siRNA or Hs_VDAC1_1HP_siRNA (Qiagen) using HiPerFect® transfection reagent (Qiagen).

### Statistics

Statistical analyses were conducted using analysis of variance for multiple comparisons and Student's *t* test for comparing two groups.

## RESULTS

*PQ Produces $O_2^-$ in an NADH-dependent Manner*—We first investigated whether PQ produced ROS on mitochondria in HeLa cells. We detected $O_2^-$ on the mitochondria using MitoSOX fluorogenic dye (Fig. 1*A*). Whereas only slight fluorescence was detected on the mitochondria in cells exposed to normal conditions, highly intense levels of fluorescence were observed when the cells were exposed to PQ. Fluorescence was reduced to the control level with the addition of BQ, a scavenger of $O_2^-$. In isolated rat liver mitochondria, we detected the NADH-dependent production of $H_2O_2$ by PQ using DCFH fluorescent dye (Fig. 1*B*). Although the fluorescence intensity did not change when PQ or NADH alone was added to the isolated mitochondria, the addition of PQ in combination with NADH raised the intensity of fluorescence in the mitochondria. BQ suppressed this augmentation. We also observed that the co-administration of PQ and NADH led to a loss of structural integrity of the isolated mitochondria, and SOD suppressed this damage (Fig. 1*C*). Furthermore, Torolox®, an $O_2^-$ scavenger, significantly increased the survival rates of HeLa cells exposed to PQ ($p < 0.05$, Fig. 1*D*). These results indicated that PQ produced $O_2^-$ in an NADH-dependent manner in mitochondria and damaged mitochondria followed by cell death.

*VDAC1 Is Responsible for NDAH-PQ Oxidoreductase Activity*—To reveal the components involved in this activity, we performed two-step extraction with Triton X-100, deoxycholate followed by SDS/Igepal CA-630 from the outer membrane and analyzed SDS/Igepal extract. The extract oxidized NADH, but not NADPH, by the addition of PQ (Fig. 2*A*), and $O_2^-$ was produced in a PQ dose-dependent manner (Fig. 2*B*). The NADH oxidation activity was 4.4 times that of the Triton X-100/deoxycholate extract (data not shown). To ascertain whether or not VDAC protein is involved in NADH-PQ oxidoreductase activity, we examined the effects of VDAC inhibitors on this activity (Fig. 3*A*). $O_2^-$ production by the extract from the outer membrane mixed with PQ and NADH was significantly inhibited by DIDS, an anion channel inhibitor, or anti-VDAC1 mAb, but such inhibition was not observed with exposure of the extract to normal mouse IgG. When the extract was immunoprecipitated with anti-VDAC1 mAb, the activity in the supernatant was lower than that observed with the administration of normal IgG (Fig. 3*B*). Furthermore, we confirmed that DIDS and anti-VDAC1 mAb inhibited the production of $O_2^-$ and also inhibited the breakdown of isolated mitochondria exposed to PQ and NADH (Fig. 3, *C* and *D*). These results suggest that VDAC1 is responsible for NADH-PQ oxidoreductase activity.

*VDAC1 Is Component of NADH-PQ Oxidoreductase*—Because, VDAC1 protein was more highly concentrated in the SDS/Igepal extract than in the Triton X-100/deoxycholate extract (Fig. 4*A*), we investigated whether or not VDAC1 protein is contained in the oxidoreductase. We purified the active fraction from the SDS/Igepal extract using DEAE chromatography and carried out zymography on the fraction by native PAGE in blue tetrazolium solution with PQ and NADH. A

Downloaded from www.jbc.org at EHIME UNIVERSITY, on October 22, 2009

Supplemental Material can be found at:
http://www.jbc.org/content/suppl/2009/08/28/M109.033431.DC1.html



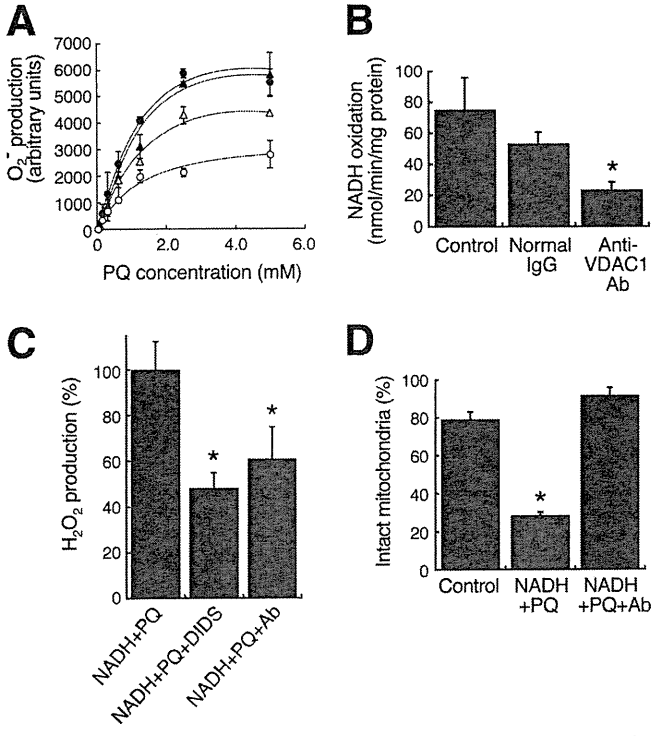


FIGURE 3. **Participation of VDAC1 in the NADH-PQ oxidoreductase activity and mitochondrial damage.** *A*, $O_2^-$ production in the outer membrane extract (*closed circle*) was inhibited by DIDS (100 μM; *open circle*, $p < 0.001$, $n = 3$) and anti-VDAC1 mAb (30 μg/ml; *open triangle*, $p < 0.05$, $n = 3$). *Closed triangle*, treated with normal IgG (30 μg/ml). *Error bars* represent S.D. ($n = 3$). *B*, the extract was immunoprecipitated with anti-VDAC1 mAb or normal IgG, and the NADH-oxidation activity of the supernatants was measured. *Control*, no treatment. *, $p < 0.01$, *versus* control. *Error bars* represent S.D. ($n = 3$). *C*, $H_2O_2$ production in isolated mitochondria by PQ (10 mM) co-administered with NADH (2 mM) was estimated by DCF florescence method. DIDS (100 μM) and anti-VDAC1 mAb (9 μg/ml) were inhibited $H_2O_2$ production. *, $p < 0.001$ with respect to the control. Each point is the mean of triplicate experiments. *Error bars* represent S.E. *D*, effects of anti-VDAC1 antibody on the NADH-PQ-dependent breakage of mitochondria were estimated. Isolated mitochondria were ruptured by the co-administration of PQ (3 mM) and NADH (2 mM), whereas the addition of anti-VDAC1 mAb (9 μg/ml) protected the mitochondria from such breakage. *, $p < 0.01$ *versus* the control. Each point is the mean of triplicate experiments. *Error bars* represent S.E.

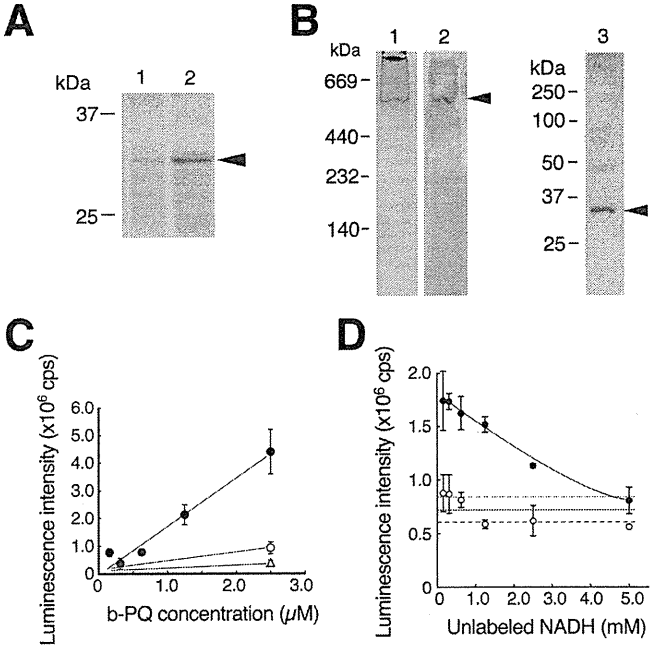


FIGURE 4. **VDAC1 is a component of NADH-PQ oxidoreductase.** *A*, extracts obtained from the mitochondrial outer membrane by treatment with Triton X-100/deoxycholate (*lane 1*) or SDS/ Igepal CA-630 (*lane 2*) were run on SDS-PAGE, and the results were analyzed by Western blotting with anti-VDAC1 mAb. VDAC1 protein was detected by the mAb (*arrowhead*). *B*, DEAE fractions from the extracts containing oxidoreductase activity were examined by zymography with NADH and PQ in blue tetrazolium solution (*lane 1*). The active band was consistent with the anti-VDAC1 mAb-detected band (*lane 2*, *arrowhead*), and this band was excised and subjected to Western blot analysis using anti-VDAC1 mAb (*lane 3*; the *arrowhead* indicates VDAC1 protein). *C*, direct binding to VDAC1 was assayed using biotinylated (*b-*) PQ (*closed circle*) in competition with non-labeled PQ (*open circle*, 25 μM, *open triangle*, 250 μM). *Error bars* represent S.D. ($n = 3$). *D*, assay of NADH binding to the outer membrane extracts was performed. The extracts were trapped by immobilized anti-VDAC1 antibody and incubated with biotinylated $NAD^+$. Bound biotinylated $NAD^+$ was reduced by exposure to non-labeled NADH ($p < 0.01$, *closed circles*). When normal IgG was used for trapping, no NADH competition was detected (*open circles*). *Broken lines* represent 95% confidence interval of the control value. *Error bars* represent S.D. ($n = 3$).

major reactive band stained with dark blue diformazan, a form of blue tetrazolium reduced by $O_2^-$, appeared at 500 kDa (Fig. 4*B*, *lane 1*); this band was recognized using anti-VDAC1 mAb (*lane 2*). Next, the excised band was examined by Western blot analysis with SDS-PAGE using anti-VDAC1 mAb. The antibody recognized a band at 31 kDa, the size of VDAC1 (*lane 3*). Because several proteins were detected in the reactive band by SDS-PAGE followed by silver staining (data not shown), the oxidoreductase may be a complex containing the VDAC1 protein. To confirm the direct interaction of VDAC1 with PQ, we performed a binding assay using recombinant VDAC1 protein and biotinylated PQ (Fig. 4*C*). We detected biotinylated PQ dose-dependently bound to the VDAC1 protein, and excess non-labeled PQ competed for the binding. Next, we examined the interaction of VDAC1 with NADH using biotinylated $NAD^+$. Whereas the biotinylated $NAD^+$ was not found to bind to the recombinant VDAC1 protein, which was immobilized by anti-VDAC1 mAb (data not shown), we did detect binding of the biotinylated $NAD^+$ using the SDS/Igepal extract instead of the VDAC1 protein (Fig. 4*D*). These results were compatible with the absence of NADH-PQ oxidoreductase activity in the recombinant VDAC1 protein or purified VDAC from rat liver mitochondria (data not shown). The present results indicate that VDAC1 is involved in NADH-PQ oxidoreductase activity as a component of the PQ binding site.

*VDAC1 Is Responsible for the Cytotoxicity of PQ*—Finally, we determined whether the amount of VDAC1 protein in cells affects PQ sensitivity. We obtained stable transfectants of HeLa cells overexpressing VDAC1; these cells had 2.2 times the VDAC1 protein content of control cells (Fig. 5*A*). When treated with PQ, these VDAC1-overexpressing cells showed 2.0 times the intracellular production of $H_2O_2$ compared with that of control cells (Fig. 5*B*). The $IC_{50}$ of control cells exposed to PQ was 72.3 μM, and this value fell to 30.7 μM in the VDAC1-overexpressing cells (Fig. 5*C*). When HeLa cells were transfected with VDAC1 siRNA, almost no VDAC1 protein was synthesized (Fig. 6*A*). Mitochondria were isolated from these cells, and the NADH-PQ dependent $H_2O_2$ production was estimated (Fig. 6*B*). The production of $H_2O_2$ on the mitochondria from knockdown cells was reduced to endogenous levels. The sur-



Downloaded from www.jbc.org at EHIME UNIVERSITY, on October 22, 2009

Supplemental Material can be found at:
http://www.jbc.org/content/suppl/2009/08/28/M109.033431.DC1.html



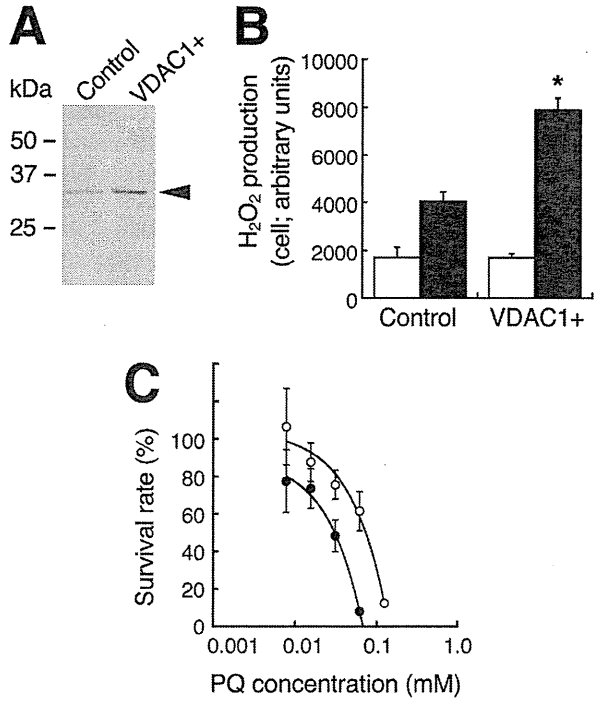


FIGURE 5. **Effects of VDAC1 overexpression on the PQ-dependent $H_2O_2$ production and the cytotoxicity in HeLa cells.** *A*, lysates from VDAC1-overexpressing cells were subjected to Western blot analysis with anti-VDAC1 mAb. *Control*, cells transfected with empty vector; *VDAC+*, cells transfected with the vector bearing *vdac1* cDNA. *B*, $H_2O_2$ production by PQ in VDAC1-overexpressing cells (*VDAC1+*) was higher than that of control cells (*, $p < 0.001$). *Light bars*, no treatment; *dark bars*, exposure to 1 mM PQ. *Error bars* represent S.D. ($n = 3$). *C*, the survival rates of VDAC1-overexpressing HeLa cells (*closed circle*) were lower than those of controls (open circle; $p < 0.001$). *Error bars* represent S.E. of triplicate experiments.

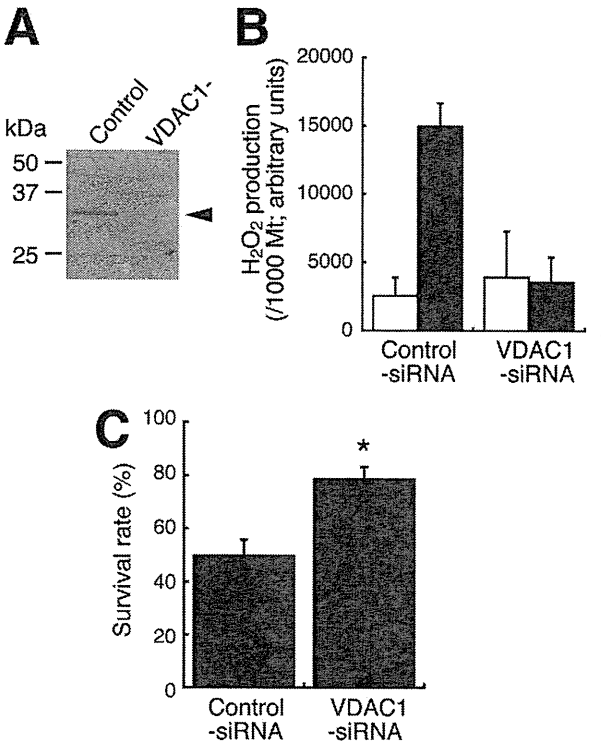


FIGURE 6. **Effects of VDAC1 knockdown on the PQ-dependent $H_2O_2$ production and the cytotoxicity in HeLa cells.** *A*, lysates from knockdown cells were subjected to Western blot analysis with anti-VDAC1 mAb. *Control*, cells transfected with the control siRNA; *VDAC−*, cells transfected with VDAC1 siRNA. The *arrowheads* indicate VDAC1 protein. *B*, NADH-PQ-dependent $H_2O_2$ production on mitochondria isolated from VDAC1-knockdown HeLa cells was estimated by DCF assay. *Light bars*, mitochondria incubated with 2 mM NADH only; *dark bars*, mitochondria were incubated with 10 mM PQ and 2 mM NADH. *Error bars* represent S.D. ($n = 3$). *C*, the survival rate of VDAC1-knockdown HeLa cells (VDA1-siRNA) after 24 h of exposure to 222 μM PQ was higher than that of control cells ($p < 0.001$). *Error bars* represent S.E. of triplicate experiments.

vival rate after exposure of the VDAC1 knockdown cells to 222 μM PQ for 24 h was 79% compared with 50% in controls (Fig. 6*C*). These results indicated that VDAC1 is responsible for the cytotoxicity of PQ as an NADH-dependent oxidoreductase.

## DISCUSSION

In this study we demonstrate that a mitochondrial system, not a microsomal system, is involved in PQ poisoning; PQ produces $O_2^-$ by NADH-dependent oxidoreductase in the outer membrane of mitochondria and damages mitochondria, leading to cell death. Furthermore, we present that mitochondrial VDAC1 is responsible for this activity as a component of the PQ binding site.

We observed $O_2^-$ production on the mitochondria after administering PQ to cells using MitoSOX, an $O_2^-$-specific fluorescent dye. Additionally, we detected $H_2O_2$ production on isolated mitochondria in the presence of PQ and NADH using DCFH fluorescent dye, and BQ reduced the level of production. In a previous study we observed that cytochrome *c*, an $O_2^-$ scavenger, diminished $H_2O_2$ production on mitochondria incubated with PQ and NADH (13). Because $O_2^-$ is immediately ($10^5$ $M^{-1}s^{-1}$) converted into $H_2O_2$ in aqueous solution, DCF fluorescence demonstrating $H_2O_2$ is considered to be equivalent to a demonstration of $O_2^-$ production (13). We also indicated that PQ destroyed isolated mitochondria in the presence of NADH and that SOD suppressed this damage. Furthermore, Trolox® suppressed the toxicity of PQ in cells. We formerly reported that PQ selectively destroyed the mitochondria of pulmonary type II cells and hepatocyte *in vivo* (6, 11) and also destroyed cultured type II cells (7). These results indicate that PQ attacks mitochondria by NADH-dependent $O_2^-$ production in the course of its cytotoxicity.

In an ultrastructural study, we previously observed that NADH-dependent $O_2^-$ production by PQ occurred in the outer membrane of mitochondria (13) and demonstrated that the NADH oxidation activity by PQ in the outer membrane fraction was five times that of the inner membrane fraction (12). $O_2$ uptake on mitochondria took place with the addition of PQ and NADH (11, 12), and blue PQ radicals formed under anaerobic conditions (11). In the present study we again observed NADH oxidation and PQ radical formation in the outer membrane under anaerobic conditions (data not shown). These results indicated that an NADH-PQ oxidoreductase is localized in the outer membrane. We previously confirmed that NADH-cytochrome $b_5$ reductase, an outer membrane-localized oxidoreductase, did not participate in the PQ reduction, based on its insensitivity to anti-NADH-cytochrome $b_5$ reductase antibody and a different sensitivity to *p*-hydroxymercuribenzoate (12). We also reported that rotenone, an inhibitor of complex I in the electron

Downloaded from www.jbc.org at EHIME UNIVERSITY, on October 22, 2009

Supplemental Material can be found at:
http://www.jbc.org/content/suppl/2009/08/28/M109.033431.DC1.html



transport chain, did not inhibit NADH-dependent PQ reduction (11, 12). Intriguingly, we find that VDAC1 is a constituent of the NADH-PQ oxidoreductase. VDAC1 is a small, abundant, pore-forming protein found in the outer membranes of all eukaryotic mitochondria and plays an important role in the passage of adenine nucleotides, $Ca^{2+}$, and other metabolites through the outer membrane (27). In addition, VDAC1 located at contact sites between the outer and inner membranes forms permeability transition pores (PTPs) with the adenine nucleotide transporter, cyclophilin D, and other proteins (27). It is unknown whether PTP proteins besides VDAC1 participate in the NADH-PQ oxidoreductase activity; thus, it will still be necessary to investigate their involvement with PTP proteins.

Extramitochondrial oxidative stress induces PTP openings via VDAC protein without damage to the inner membrane (27). PQ does not penetrate mitochondrial membrane (28), and $O_2^-$ production by PQ occurs on the outer surface of the outer membrane (13). Furthermore, we demonstrated the binding of PQ to VDAC1 protein by biotinylated PQ and the inhibition of PQ-dependent mitochondrial breakage by anti-VDAC1 mAb. These results indicated that the breakage of mitochondria by PQ occurred through VDAC1. The binding mechanism of PQ, a cation molecule, to VDAC1 remains unknown. It has been reported that NADH increased the voltage dependence of VDAC and reduced the conductance of the outer membrane (29, 30). The ion selectivity of VDAC changed from anions to cations when conductance decreased (31). NADH may, therefore, affect the binding of PQ to VDAC1. Baker *et al.* (16) reported that VDAC1 localized in the plasma membrane functions as NADH-ferricyanide reductase and that VDAC1 has a putative $NAD^+$ binding motif. Yehezkel *et al.* (32) demonstrated that VDAC purified from rat liver mitochondria had nucleotide binding sites bound to ATP; however, NADH did not bind them. As in a previous study (Hirai *et al.* (11), the change in conformation from the orthodox to the condensed type occurred when NADH was added to starved intact mitochondria. In addition, NADH reduced the permeability of the outer membrane to ADP (15). These results indicated that NADH affects PTP even though NADH does not bind to VDAC1 directly. Although we did not observe the direct binding of NADH to VDAC1 alone, we did observe the binding of biotinylated $NAD^+$ to the NADH-PQ oxidoreductase concentrated extract, which was trapped by anti-VDAC1 mAb. NADH-PQ oxidoreductase activity was inhibited by DIDS and anti-VDAC1 mAb, but recombinant VDAC1 protein or purified VDAC protein alone had no activity. Therefore, an NADH binding component is expected to be necessary to yield this activity.

Yagoda *et al.* (33) reported that VDAC2 or VDAC3 was implicated in the cytotoxicity of the anti-tumor agent erastin, which was shown to induce oxidative cell death; in particular, VDAC2 was found to bind directly to this agent. We have not yet identified the involvement of VDAC2 or VDAC3 in NADH-PQ oxidoreductase activity. It has been reported that VDAC1 is the most abundantly expressed of the three VDAC isoforms in mammalian mitochondria (34). In addition, we demonstrated a correlation between the production of $O_2^-$ and VDAC1 expression, and we observed defective $O_2^-$ production on the mitochondria isolated from VDAC1 knockdown cells. Therefore, it appears that VDAC1 participates primarily in NADH-PQ oxidoreductase activity. Recently, we found that several furanonaphthoquinones caused mitochondrial damage and the apoptosis of cancer cells by the production of ROS, and other studies revealed that VDAC1 induces ROS production by an NADH-dependent quinone reduction (17, 35). Additionally, we previously demonstrated that menadione, a naphthoquinone, was a substrate of NADH-PQ oxidoreductase (12). These previous and present results taken together suggest that the function of VDAC1 is not only to serve as a channel but also to function as part of an oxidoreductase enzyme.

Until now, management of PQ poisoning has been directed primarily at removing PQ from the gastrointestinal tract by the use of several absorbents (activated charcoal, Fuller's Earth, etc.) and increasing its excretion from the blood by hemoperfusion (2). However, the efficacy of these treatments is poor. Our results indicated that $O_2^-$ production by a VDAC-containing mitochondrial system is responsible for PQ poisoning. DIDS and anti-VDAC1 antibody inhibited NADH-PQ oxidoreductase activity, mitochondrial $O_2^-$ production, and the breakage of mitochondria by PQ. Furthermore, PQ cytotoxicity was suppressed in VDAC1-knockdown cells. These results suggest that specific VDAC inhibitors can be therapeutic agents of PQ poisoning.

*Acknowledgment—We are grateful to Mayumi Mitani for secretarial assistance.*

## REFERENCES

1. Wesseling, C., van Wendel de Joode, B., Ruepert, C., León, C., Monge, P., Hermosillo, H., and Partanen, T. J. (2001) *Int. J. Occup. Environ. Health* **7,** 275–286
2. Dinis-Oliveira, R. J., Duarte, J. A., Sánchez-Navarro, A., Remião, F., Bastos, M. L., and Carvalho, F. (2008) *Crit. Rev. Toxicol.* **38,** 13–71
3. McCormack, A. L., Thiruchelvam, M., Manning-Bog, A. B., Thiffault, C., Langston, J. W., Cory-Slechta, D. A., and Di Monte, D. A. (2002) *Neurobiol. Dis.* **10,** 119–127
4. Baldwin, R. C., Pasi, A., MacGregor, J. T., and Hine, C. H. (1975) *Toxicol. Appl. Pharmacol.* **32,** 298–304
5. Bus, J. S., Cagen, S. Z., Olgaard, M., and Gibson, J. E. (1976) *Toxicol. Appl. Pharmacol.* **35,** 501–513
6. Hirai, K., Witschi, H., and Côté, M. G. (1985) *Exp. Mol. Pathol.* **43,** 242–252
7. Wang, G. Y., Hirai, K., and Shimada, H. (1992) *J. Electron Microsc. (Tokyo)* **41,** 181–184
8. Yang, W., and Tiffany-Castiglioni, E. (2005) *J. Toxicol. Environ. Health A* **68,** 1939–1961
9. St. Clair, D. K., Oberley, T. D., and Ho, Y. S. (1991) *FEBS Lett.* **293,** 199–203
10. Oliver, P. D., and Newsome, D. A. (1992) *Invest. Ophthalmol. Vis. Sci.* **33,** 1909–1918
11. Hirai, K., Ikeda, K., and Wang, G. Y. (1992) *Toxicology* **72,** 1–16
12. Shimada, H., Hirai, K., Simamura, E., and Pan, J. (1998) *Arch Biochem. Biophys* **351,** 75–81
13. Hirai, K. I., Pan, J., Shimada, H., Izuhara, T., Kurihara, T., and Moriguchi, K. (1999) *J. Electron Microsc. (Tokyo)* **48,** 289–296
14. Shimada, H., Furuno, H., Hirai, K., Koyama, J., Ariyama, J., and Simamura, E. (2002) *Arch. Biochem. Biophys.* **402,** 149–157
15. Lee, A. C., Xu, X., and Colombini, M. (1996) *J. Biol. Chem.* **271,** 26724–26731
16. Baker, M. A., Lane, D. J., Ly, J. D., De Pinto, V., and Lawen, A. (2004) *J. Biol. Chem.* **279,** 4811–4819



The Journal of Biological Chemistry ASBMB JBC

Downloaded from www.jbc.org at EHIME UNIVERSITY, on October 22, 2009

Supplemental Material can be found at:
http://www.jbc.org/content/suppl/2009/08/28/M109.033431.DC1.html



17. Simamura, E., Hirai, K., Shimada, H., Koyama, J., Niwa, Y., and Shimizu, S. (2006) *Cancer Biol. Ther.* **5,** 1523–1529
18. Ariyama, J., Shimada, H., Aono, M., Tsuchida, H., and Hirai, K. I. (2000) *Intensive Care Med.* **26,** 981–987
19. Nakayama, S., Sakuyama, T., Mitaku, S., and Ohta, Y. (2002) *Biochem. Biophys. Res. Commun.* **290,** 23–28
20. Saotome, K., Morita, H., and Umeda, M. (1989) *Toxicol. In Vitro* **3,** 317–321
21. Teraoka, K., and Matsui, S. (1999) *Nippon Rinsho.* **57,** (suppl.) 784–788
22. Narita, M., Shimizu, S., Ito, T., Chittenden, T., Lutz, R. J., Matsuda, H., and Tsujimoto, Y. (1998) *Proc. Natl. Acad. Sci. U.S.A.* **95,** 14681–14686
23. Sawasaki, T., Ogasawara, T., Morishita, R., and Endo, Y. (2002) *Proc. Natl. Acad. Sci. U.S.A.* **99,** 14652–14657
24. Sawasaki, T., Kamura, N., Matsunaga, S., Saeki, M., Tsuchimochi, M., Morishita, R., and Endo, Y. (2008) *FEBS Lett.* **582,** 221–228
25. Sawasaki, T., Gouda, M. D., Kawasaki, T., Tsuboi, T., Tozawa, Y., Takai, K., and Endo, Y. (2005) *Methods Mol. Biol.* **310,** 131–144
26. Sawasaki, T., Hasegawa, Y., Tsuchimochi, M., Kamura, N., Ogasawara, T., Kuroita, T., and Endo, Y. (2002) *FEBS Lett.* **514,** 102–105
27. Crompton, M. (1999) *Biochem. J.* **341,** 233–249
28. Gage, J. C. (1968) *Biochem. J.* **109,** 757–761
29. Lee, A. C., Zizi, M., and Colombini, M. (1994) *J. Biol. Chem.* **269,** 30974–30980
30. Zizi, M., Byrd, C., Boxus, R., and Colombini, M. (1998) *Biophys. J.* **75,** 704–713
31. Vyssokikh, M., and Brdiczka, D. (2004) *Mol. Cell. Biochem.* **256–257,** 117–126
32. Yehezkel, G., Hadad, N., Zaid, H., Sivan, S., and Shoshan-Barmatz, V. (2006) *J. Biol. Chem.* **281,** 5938–5946
33. Yagoda, N., von Rechenberg, M., Zaganjor, E., Bauer, A. J., Yang, W. S., Fridman, D. J., Wolpaw, A. J., Smukste, I., Peltier, J. M., Boniface, J. J., Smith, R., Lessnick, S. L., Sahasrabudhe, S., and Stockwell, B. R. (2007) *Nature* **447,** 864–868
34. Yamamoto, T., Yamada, A., Watanabe, M., Yoshimura, Y., Yamazaki, N., Yoshimura, Y., Yamauchi, T., Kataoka, M., Nagata, T., Terada, H., and Shinohara, Y. (2006) *J. Proteome Res.* **5,** 3336–3344
35. Simamura, E., Shimada, H., Ishigaki, Y., Hatta, T., Higashi, N., and Hirai, K. I. (2008) *Anat. Sci. Int.* **83,** 261–266

Downloaded from www.jbc.org at EHIME UNIVERSITY, on October 22, 2009

*Biosci. Biotechnol. Biochem.*, **73** (7), 1661–1664, 2009

*Note*

# Construction of a Protein Library of Arabidopsis Transcription Factors Using a Wheat Cell-Free Protein Production System and Its Application for DNA Binding Analysis

Akira NOZAWA,[1,2] Yuko MATSUBARA,[1] Yoshinori TANAKA,[1] Hirotaka TAKAHASHI,[1] Tatsuya AKAGI,[1] Motoaki SEKI,[3] Kazuo SHINOZAKI,[4] Yaeta ENDO,[1,2,†] and Tatsuya SAWASAKI[1,2,†]

[1]*Cell-Free Science and Technology Research Center, and Venture Business Laboratory, Ehime University, 3 Bunkyo-cho, Matsuyama, Ehime 790-8577, Japan*
[2]*Systems and Structural Biology Center, RIKEN, 1-7-22 Suehiro-cho, Tsurumi-ku, Yokohama, Kanagawa 230-0045, Japan*
[3]*Plant Genomic Network Research Team, Plant Functional Genomics Research Group, RIKEN Plant Science Center, 1-7-22 Suehiro-cho, Tsurumi-ku, Yokohama, Kanagawa 230-0045, Japan*
[4]*Gene Discovery Research Team, Gene Discovery Research Group, RIKEN Plant Science Center, 3-1-1 Koyadai, Tsukuba, Ibaraki 305-0074, Japan*

Received January 9, 2009; Accepted February 19, 2009; Online Publication, July 7, 2009
[doi:10.1271/bbb.90026]

**We created a protein library consisting of 647 Arabidopsis transcription factors (TFs) using a wheat cell-free system. The quality of proteins in the library was checked by binding assay of bZIP family proteins. Screening of TFs binding to 5′-regulatory regions of *FLC* and *LFY* was conducted using the library, and MYB67 and GBF1 were found to be binding factors.**

**Key words:** Arabidopsis; wheat cell-free protein production system; transcription factor

The completion of entire genome sequences of various organisms has resulted in the identification of large numbers of novel genes.[1)] The challenge ahead is to gain information about the function of these novel genes. Currently, significant effort is devoted to understanding the roles of a gene by analyzing its expression pattern or by analyzing phenotypes of the gene-specific disruption mutant. In addition to this information, biochemical characterization of the protein encoded by the gene is essential for understanding its precise function. However, only slight progress has been made in the large-scale biochemical characterization of proteins, especially at the genome-wide level. To establish a proteomics approach for the characterization of proteins, it is necessary to meet three requirements, availability of i) a wide variety of proteins, ii) sufficient amounts of proteins, and iii) functionally folded proteins.

Transcription factors (TFs) play crucial roles in almost all biological processes. The Arabidopsis genome encodes more than 1,500 transcription factors.[2)] These TFs are classified into various TF families according to the distinct type of DNA binding domains, such as AP2/EREBP, bZIP, HD-ZIP, Myb, MADS, and several classes of zinc finger proteins. TFs control gene expression by binding to specific DNA sequences in the genome. However, the number of TFs whose binding sequences have been confirmed by biochemical analyses is limited, mainly because of the difficulty in obtaining sufficient amounts of purified TF proteins, as they are expressed in small quantities in the cell. Overexpression of recombinant TF proteins in cells is generally difficult because overexpression of TFs often inhibits host cell physiology. Here, we constructed an Arabidopsis TF protein library based on our wheat cell-free protein synthesis system.[3,4)] For evaluation of the library, we performed several biochemical analyses. Our results indicate that the cell-free based Arabidopsis TF protein library is a powerful tool in the large-scale functional analysis of TFs.

Genome analysis revealed at least 1,500 TFs, classifiable into 45 families, in the Arabidopsis genome.[2)] Out of these, cDNA clones of 1,076 TFs were in the RIKEN Arabidopsis full-length (RAFL) clone collection.[5)] *Escherichia coli* cells harboring the cDNA clones were inoculated individually in 96-well plates, and the plates were then incubated for 48 h at 37 °C. DNA templates for transcription were prepared from each *E. coli* clone using the split-primer polymerase chain reaction (PCR) method, as described in our previous reports.[4,6)] Finally, we prepared a total of 705 DNA templates for transcription from the 1,076 RAFL clones. mRNAs were prepared from each amplified DNA template, and the synthesized mRNAs were used for protein synthesis by the bilayer method.[7)] Following this protocol, we created a protein library, AtTF, consisting of 647 synthesized Arabidopsis TFs. The mean values for the amount (concentration) and solubility of all synthesized TFs were 1 μM and 72% respectively (Fig. 1A). The size of each protein synthesized was confirmed by SDS-polyacrylamide gel electrophoresis (PAGE) analysis (data not shown). We did not observe any major difference among the families as far as protein synthesis and solubility were concerned. All the families included both

† To whom correspondence should be addressed. Yaeta ENDO, Fax: +81-89-927-9941; E-mail: yendo@eng.ehime-u.ac.jp; Tatsuya SAWASAKI, Fax: +81-89-927-9941; E-mail: sawasaki@eng.ehime-u.ac.jp

*Abbreviations*: PAGE, polyacrylamide gel electrophoresis; RAFL, RIKEN Arabidopsis full-length; PCR, polymerase chain reaction; TF, transcription factor; TRR, transcription regulatory region

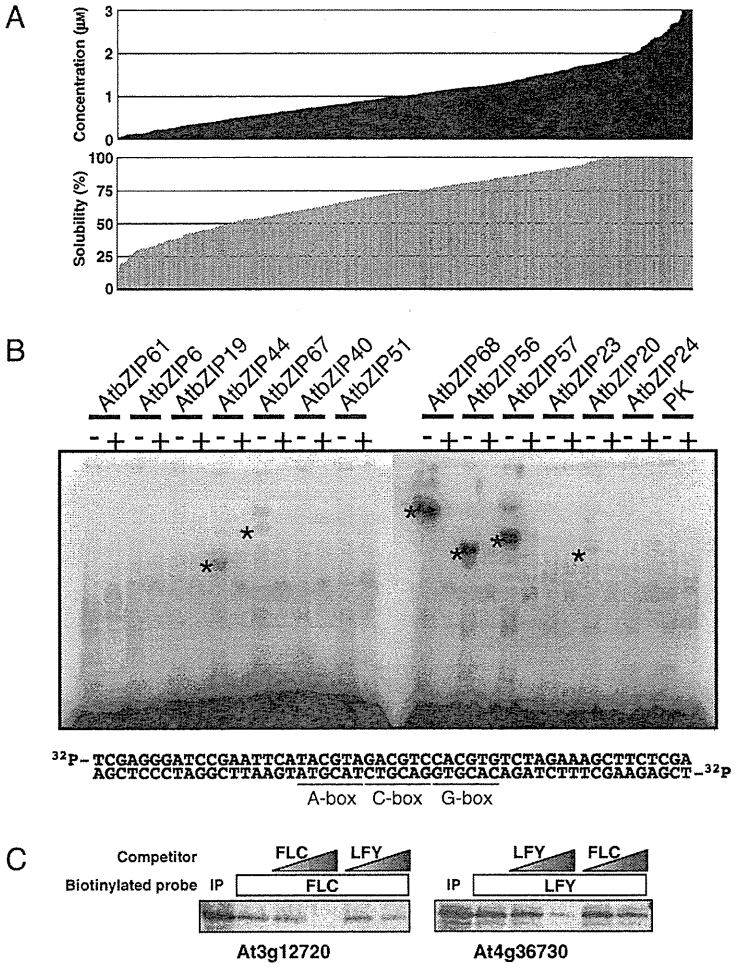


**Fig. 1.** Construction of a Protein Library of Arabidopsis Transcription Factors and Its Application to DNA Binding Assay.

A, High-throughput production of Arabidopsis TF proteins by the wheat germ cell-free protein synthesis system. Arabidopsis TF proteins (n = 647) were synthesized using the wheat germ cell-free system, as described in the text. The concentration (μM) and solubility of these synthesized TF proteins are shown in separate panels. Results are arrayed so that the value of each parameter increases from left to right in each panel. B, DNA binding analysis of the bZIP proteins. The [$^{32}$P]-labeled DNA probe (shown at the bottom of the figure) and an indicated bZIP protein were incubated in the presence (+) and the absence (−) of a competitor (10-fold excess of the non-labeled probe). After 30 min of incubation, the samples were subjected to PAGE. Asterisks indicate shifted bands of DNA-protein complex. Lanes of PK show results using a protein kinase, GSK1 (negative control). The nucleotide sequences of the oligonucleotides used as the probe are also shown. The sequences of the A-, C-, and G-boxes are underlined. C, Screening of TF proteins. TF proteins synthesized from cDNA clones (At3g12720 and At4g36730) were incubated with the respective biotinylated promoter probes in the presence and the absence of non-labeled competitor DNA fragment (*FLC* or *LFY*, 5- and 10-fold excess respectively). After 30 min, the samples were pulled down with streptavidin-conjugated magnetic beads, subjected to SDS–PAGE, and detected by autoradiography. IP, proteins inputted to this assay.

poorly-synthesized and well-synthesized TF proteins. There was no TF family from which no members could be synthesized using this cell-free protein synthesis system. These results suggest that our cell-free protein synthesis system can synthesize sufficient quantities of good-quality Arabidopsis TFs for functional analysis.

To determine whether these synthesized TF proteins can be used for functional analysis, we demonstrated two independent DNA binding assays using this protein library. First we examined the DNA binding activity of the bZIP TFs in this library. bZIP TFs have a basic region that binds to the DNA and a leucine zipper dimerization motif.[8] Proteins with bZIP domains are present in all eukaryotes analyzed to date. Some of the bZIP TFs, such as Jun/Fos or CREB, have been extensively studied in animals, and they serve as models for understanding TF-DNA interactions, ternary complex formation, and post-translational modifications.[8] Plant bZIP proteins bind to DNA sequences with an ACGT core, preferentially to A-box (TACGTA), C-box (GACGTC), and G-box (CACGTG).[9] Seventy-five bZIP transcription factors were found in the Arabidopsis genome, and they were classified into 11 groups.[8] In this study, 54 bZIP proteins were synthesized using the cell-free protein synthesis system. Among them, 45 bZIP proteins (60% of the family), concentration of which was approximately 0.4 μM, were used for the binding assay. The DNA-binding ability of each synthesized TF was detected by gel retardation assay using a specific DNA fragment that contained the A-, C-, and G-box. Gel retardation assay was conducted as previously described.[10] DNA-binding ability was confirmed for 19 out of 45 bZIPs proteins. The representative results of gel retardation assay are shown in Fig. 1B. The results of the DNA-binding assay are summarized in Table 1. bZIP proteins belonging to A, C, D, G, H, and S groups were reported to bind DNA sequences with an ACGT core.[8,11–14] Among them, binding of groups A,

**Table 1.** Results of DNA Binding Assay for the bZIP Family Proteins in Arabidopsis

| Name | AGI code | G[a] | Published name | DNA binding | Name | AGI code | G | Published name | DNA binding |
|---|---|---|---|---|---|---|---|---|---|
| AtbZIP40 | At1g03970 | A | GBF4 | nd[b] | AtbZIP68 | At1g32150 | G | . | YES |
| AtbZIP35 | At1g49720 | A | ABF1 | YES | AtbZIP55 | At2g46270 | G | GBF3 | YES |
| AtbZIP39 | At2g36270 | A | ABI5 | nd | AtbZIP54 | At4g01120 | G | GBF2 | YES |
| AtbZIP12 | At2g41070 | A | DPBF4 | YES | AtbZIP41 | At4g36730 | G | GBF1 | YES |
| AtbZIP67 | At3g44460 | A | DPBF2 | YES | AtbZIP56 | At5g11260 | H | HY5 | YES |
| AtbZIP66 | At3g56850 | A | AREB3 | YES | AtbZIP69 | At1g06070 | I | . | nd |
| AtbZIP37 | At4g34000 | A | ABF3 | YES | AtbZIP52 | At1g06850 | I | . | nd |
| AtbZIP13 | At5g44080 | A | . | nd | AtbZIP51 | At1g43700 | I | VIP1 | nd |
| AtbZIP17 | At2g40950 | B | . | nd | AtbZIP59 | At2g31370 | I | PosF21 | nd |
| AtbZIP28 | At3g10800 | B | . | nd | AtbZIP18 | At2g40620 | I | . | nd |
| AtbZIP25 | At3g54620 | C | . | nd | AtbZIP29 | At4g38900 | I | . | nd |
| AtbZIP9 | At5g24800 | C | BZO2H2 | nd | AtbZIP44 | At1g75390 | S | . | YES |
| AtbZIP63 | At5g28770 | C | . | nd | AtbZIP2 | At2g18160 | S | GBF5 | YES |
| AtbZIP22 | At1g22070 | D | TGA3 | nd | AtbZIP6 | At2g22850 | S | . | nd |
| AtbZIP46 | At1g68640 | D | Perianthia | nd | AtbZIP53 | At3g62420 | S | . | YES |
| AtbZIP50 | At1g77920 | D | . | YES | AtbZIP11 | At4g34590 | S | GBF6 | YES |
| AtbZIP20 | At5g06950 | D | TGA2 | YES | AtbZIP3 | At5g15830 | S | . | YES |
| AtbZIP26 | At5g06960 | D | TGA5 | YES | AtbZIP1 | At5g49450 | S | . | nd |
| AtbZIP57 | At5g10030 | D | TGA4 | YES | AtbZIP62 | At1g19490 | — | . | nd |
| AtbZIP47 | At5g65210 | D | TGA1 | YES | AtbZIP60 | At1g42990 | — | . | nd |
| AtbZIP34 | At2g42380 | E | . | nd | | | | | |
| AtbZIP61 | At3g58120 | E | . | nd | | | | | |
| AtbZIP23 | At2g16770 | F | . | nd | | | | | |
| AtbZIP24 | At3g51960 | F | . | nd | | | | | |
| AtbZIP19 | At4g35040 | F | . | nd | | | | | |

[a]group
[b]not detected

D, G, H, and S in the bZIP family with DNA sequences containing the ACGT core was confirmed (Table 1). On the other hand, no binding of group C proteins was observed. It has been reported that group C proteins in the bZIP family have conserved phosphorylation sites,[8] and that a maize group C bZIP protein, Opaque2, is modified by phosphorylation.[15] Hence group C proteins may need some modification such as phosphorylation for binding.

Transcription is controlled by binding of TFs to the transcription regulatory region (TRR) in the 5′-upstream region of a gene. Thus, for better understanding of the gene expression network, it is important to analyze the binding of a TF to the TRR of a gene. Initiation of flowering is regulated by many genes. Among these, the *FLC* and *LFY* genes are known to be important negative and positive regulators respectively.[16,17] Next we used the upstream regions of the *FLC* (At5g10140) and *LFY* (At5g61850) genes as the target TRR sequences and searched for the TFs binding to these TRRs. For this purpose, biotinylated target TRR fragments containing the respective 5′-regulatory regions (300 bp, encompassing the −450 to −150 bp upstream region from the start codon of each gene) were generated by PCR using 5′-biotin-labeled primers, and randomly selected 192 TFs were synthesized by a cell-free protein synthesis system using [$^{14}$C]leucine. We divided the $^{14}$C-labeled TFs into eight groups, each of which contained 24 different TFs. Each group of TFs was then mixed and incubated with one of the biotin-labeled target TRR fragments. After incubation, the target TRR fragments were pulled down using streptavidin-conjugated magnetic beads. The beads were washed 3 times and then subjected to SDS–PAGE analysis. In our search for the TFs binding to the *FLC* TRR fragment, specific binding of a 44 kDa protein to the fragment was observed in a TF group (data not shown). Among the 24 TFs that were mixed and used in the binding assay in the group, three TFs had predicted molecular masses of about 44 kDa. The binding activities of these three candidates to the *FLC* fragment were individually examined by competition assay. The candidate proteins were incubated with a biotinylated *FLC* fragment in the presence and the absence of a non-labeled competitor DNA fragment, and finally the At3g12720 product (MYB67) was found bind specifically to the TRR region of the *FLC* gene (Fig. 1C). Following the same assay protocol, a protein synthesized from clone At4g36730 (G-box binding factor 1, GBF1) was found to be a specific binding protein for the *LFY* TRR fragment (Fig. 1C). MYB67 and GBF1 belong to the MYB and bZIP families respectively. Typical binding sequences for MYB ((C/T)AAC(T/G)G) and bZIP (G-box: CACGTG) TFs do not exist in TRR fragments used in these experiments, but similar sequences, TAAATG (−314 to −319) and CACATT (−201 to −206), were found in the *FLC* and *LFY* TRR fragments respectively. Binding of GBF1 to CACATT in the *LFY* TRR fragment was confirmed by DNA foot-printing analysis (data not shown). Although further experiments are required to determine whether MYB67 and GBF1 do in fact bind to those sequences in *FLC* and *LFY* TRR respectively *in vivo*, these results suggest that our TF protein library may help in large-scale screening for isolation of TFs that bind to the TRR of target genes. Furthermore, the result that a bZIP TF, GBF1, binds to a sequence not identical to the A-, C-, or G-boxes suggests that the bZIP TFs for which we did not detect binding activity with the A-, C-, or G-boxes in this study might also recognize similar sequences to those elements.

For genome-wide biochemical analysis, large-scale synthesis of proteins has so far been a technological bottleneck. Methodologically, it is impossible to achieve genome-scale synthesis of proteins by conventional methods using living cells. In contrast, our cell-free protein synthesis system from wheat embryo is very suitable for the large-scale production of proteins. We created a protein library consisting of 647 Arabidopsis TFs using the cell-free system in this study. Using the TF library, we demonstrated DNA-binding assay of bZIP TFs and screening of TF binding to the TRR of *FLC* and *LFY*. These results indicate that the quality of the protein library is sufficient for large-scale biochemical characterization. The cell-free based protein library might become a promising tool in genome-wide biochemical analysis. Recently, we also succeeded in establishing a protein microarray system based on this cell-free protein synthesis system.[18] We hope that appropriate use of these methods will accelerate the progress of the genome-wide biochemical analysis of proteins.

## Acknowledgments

This work was partially supported by the program of Special Coordination Funds for Promoting Science and Technology of the Ministry of Education, Culture, Sports, Science, and Technology of Japan (financial support to T.S. and Y.E.).

## References

1) International Human Genome Sequencing Consortium, *Nature*, **409**, 860–921 (2001).
2) Riechmann JL, Heard J, Martin G, Reuber L, Jiang CZ, Keddie J, Adam L, Pineda O, Ratcliffe OJ, Samaha RR, Creelman R, Pilgrim M, Broun P, Zhang JZ, Ghandehari D, Sherman BK, and Yu GL, *Science*, **290**, 2105–2110 (2000).
3) Madin K, Sawasaki T, Ogasawara T, and Endo Y, *Proc. Natl. Acad. Sci. USA*, **97**, 559–564 (2000).
4) Sawasaki T, Ogasawara T, Morishita R, and Endo Y, *Proc. Natl. Acad. Sci. USA*, **99**, 14652–14657 (2002).
5) Seki M, Narusaka M, Kamiya A, Ishida J, Satou M, Sakurai T, Nakajima M, Enju A, Akiyama K, Oono Y, Muramatsu M, Hayashizaki Y, Kawai J, Carninci P, Itoh M, Ishii Y, Akazawa T, Shibata K, Shinagawa A, and Shinozaki K, *Science*, **296**, 141–145 (2002).
6) Sawasaki T, Morishita R, Gouda MD, and Endo Y, *Methods Mol. Biol.*, **375**, 95–106 (2007).
7) Sawasaki T, Hasegawa Y, Tsuchimochi M, Kamura N, Ogasawara T, Kuroita T, and Endo Y, *FEBS Lett.*, **514**, 102–105 (2002).
8) Jakoby M, Weisshaar B, Droge-Laser W, Vicente-Carbajosa J, Tiedemann J, Kroj T, and Parcy F, *Trends Plant Sci.*, **7**, 106–111 (2002).
9) Izawa T, Foster R, Nakajima M, Shimamoto K, and Chua NH, *Plant Cell*, **6**, 1277–1287 (1994).
10) Kobayashi T, Kodani Y, Nozawa A, Endo Y, and Sawasaki T, *FEBS Lett.*, **582**, 2737–2744 (2008).
11) Lara P, Oñate-Sánchez L, Abraham Z, Ferrándiz C, Díaz I, Carbonero P, and Vicente-Carbajosa J, *J. Biol. Chem.*, **278**, 21003–21011 (2003).
12) Satoh R, Fujita Y, Nakashima K, Shinozaki K, and Yamaguchi-Shinozaki K, *Plant Cell Physiol.*, **45**, 309–317 (2004).
13) Lee SS, Yang SH, Berberich T, Miyazaki A, and Kusano T, *Plant Biotechnol.*, **23**, 249–258 (2006).
14) Kaminaka H, Näke C, Epple P, Dittgen J, Schütze K, Chaban C, Holt III BF, Merkle T, Schäfer E, Harter K, and Dangl JL, *EMBO J.*, **25**, 4400–4411 (2006).
15) Ciceri P, Gianazza E, Lazzari B, Lippoli G, Genga A, Hoschek G, Schmidt RJ, and Viotti A, *Plant Cell*, **9**, 97–108 (1997).
16) Alexandre CA and Hennig L, *J. Exp. Bot.*, **59**, 1127–1135 (2008).
17) Sablowski R, *J. Exp. Bot.*, **58**, 899–907 (2007).
18) Sawasaki T, Kamura N, Matsunaga S, Saeki M, Tsuchimochi M, Morishita R, and Endo Y, *FEBS Lett.*, **582**, 221–228 (2008).

*Journal of Experimental Botany*, Vol. 60, No. 11, pp. 3067–3073, 2009
doi:10.1093/jxb/erp134 Advance Access publication 8 May, 2009
This paper is available online free of all access charges (see http://jxb.oxfordjournals.org/open_access.html for further details)

Journal of Experimental Botany
www.jxb.oxfordjournals.org

RESEARCH PAPER

# Isolation and identification of ubiquitin-related proteins from *Arabidopsis* seedlings

**Tomoko Igawa[1,*], Masayuki Fujiwara[1], Hirotaka Takahashi[2], Tatsuya Sawasaki[2], Yaeta Endo[2], Motoaki Seki[3], Kazuo Shinozaki[3], Yoichiro Fukao[1] and Yuki Yanagawa[1,*,†]**

[1] The Plant Science Education Unit, The Graduate School of Biological Sciences, Nara Institute of Science and Technology, 8916-5 Takayama-cho, Ikoma, Nara 630-0101, Japan
[2] Cell-Free Science and Technology Research Center, Ehime University, 3 Bunkyo-cho, Matsuyama, Ehime 790-8577, Japan
[3] RIKEN Bioresource Center, 3-1-1 Takayama-cho, Tsukuba, Ibaraki 305-0074, Japan

Received 15 December 2008; Revised 9 March 2009; Accepted 6 April 2009

## Abstract

**The majority of proteins in eukaryotic cells are modified according to highly regulated mechanisms to fulfill specific functions and to achieve localization, stability, and transport. Protein ubiquitination is one of the major post-translational modifications occurring in eukaryotic cells. To obtain the proteomic dataset related to the ubiquitin (Ub)-dependent regulatory system in *Arabidopsis*, affinity purification with an anti-Ub antibody under native condition was performed. Using MS/MS analysis, 196 distinct proteins represented by 251 distinct genes were identified. The identified proteins were involved in metabolism (23.0%), stress response (21.4%), translation (16.8%), transport (6.7%), cell morphology (3.6%), and signal transduction (1.5%), in addition to proteolysis (16.8%) to which proteasome subunits (14.3%) is included. On the basis of potential ubiquitination-targeting signal motifs, in-gel mobilities, and previous reports, 78 of the identified proteins were classified as ubiquitinated proteins and the rest were speculated to be associated proteins of ubiquitinated proteins. The degradation of three proteins predicted to be ubiquitinated proteins was inhibited by a proteasome inhibitor, suggesting that the proteins were regulated by Ub/proteasome-dependent proteolysis.**

**Key words:** *Arabidopsis* seedling, MS, ubiquitin-related protein.

## Introduction

Ubiquitin (Ub)-mediated protein modification is a critical post-translational regulatory mechanism that occurs in all eukaryotic cells. The conserved 76 amino acid polypeptide, Ub, is covalently attached to a substrate protein as a signal molecule, and this attachment leads to various outcomes. The widely known fate of ubiquitinated proteins is degradation by 26S proteasome, one specific case being that more than four Ubs comprise a multi-Ub chain via lysine (K) 48 residues (Thrower *et al.*, 2000). Other types of ubiquitination, such as mono-ubiquitination and non-canonical ubiquitination, are implicated in various cellular functions, including endocytosis, endosomal sorting, signal transduction, and DNA damage repair (reviewed by Haglund and Dikic, 2005). Ubiquitination of target proteins requires the sequential action of three enzymes: Ub-activating enzyme (E1), Ub-conjugating enzyme (E2 or UBC), and Ub ligase (E3) (Hershko and Ciechanover, 1998; Pickart, 2001). The completely sequenced *Arabidopsis* genome has enabled the prediction of plant ubiquitination enzymes. To date, the activities of two E1s (Hatfield *et al.*, 1997) and 25 E2s (Kraft *et al.*, 2005) have been experimentally proven, and 12 genes encoding UBC domains are predicted to be E2s on the basis of their sequences (Bachmair *et al.*, 2001). Similar to other organisms, *Arabidopsis* E3s are predicted to form the largest

* These authors contributed equally to this work.
† To whom correspondence should be addressed: E-mail: yyana@bs.naist.jp
Abbreviations: DET3, de-etiolated 3; FBA, fructose biphosphate aldolase-like; GAPC, glyceraldehyde-3-phosphate dehydrogenase C subunit; ORF, open reading frame; Ub, ubiquitin; V-ATPase, vacuolar $H^+$-ATPase.
© 2009 The Author(s).
This is an Open Access article distributed under the terms of the Creative Commons Attribution Non-Commercial License (http://creativecommons.org/licenses/by-nc/2.0/uk/) which permits unrestricted non-commercial use, distribution, and reproduction in any medium, provided the original work is properly cited.

family comprising more than 1400 genes (Mazzucotelli *et al.*, 2006). Furthermore, the presence of additional proteins, such as an enhancer of E2, has been reported (Yanagawa *et al.*, 2004). Clearly, numerous proteins are involved in Ub-mediated protein regulation.

To identify ubiquitinated proteins in yeasts and mammals, several proteomic approaches that utilize various purification methods and MS/MS analyses have been reported (Peng *et al.*, 2003; Hatakeyama *et al.*, 2005; Jeon *et al.*, 2007). In plants, two groups recently reported the proteomics of ubiquitinated proteins from *Arabidopsis* cell cultures and seedlings, respectively (Maor *et al.*, 2007; Manzano *et al.*, 2008). Meanwhile, a Ub-related proteome that includes both ubiquitinated proteins and their associated proteins has been reported only in human cells (Matsumoto *et al.*, 2005).

As many proteins show spatiotemporal expression during development/life cycle, it is speculated that Ub-related proteins also vary among distinct tissues at various developmental stages. Therefore, the accumulation of information of Ub-related proteins from differentiated tissues at various stages would facilitate an understanding of Ub-mediated protein regulation throughout the life cycle. In addition, to make a comparison with the reports of Maor *et al.* (2007) and Manzano *et al.* (2008) that provided useful information of ubiquitinated proteomes from non-differentiated cell cultures and *Arabidopsis* seedlings, respectively, the proteomic analysis of Ub-related proteins expressed in *Arabidopsis* seedlings was performed in this study. For the large-scale isolation of Ub-related proteins, the purification was performed under native conditions. Previous studies of *Arabidopsis* ubiquitinated proteomes utilized different Ub-binding domains (UBAs) and showed that each UBA has distinct specificity for ubiquitinated proteins (Maor *et al.*, 2007; Manzano *et al.*, 2008). In order to overcome the limited specificity for target recognition, an anti-Ub antibody was applied to isolate Ub-related proteins. This study could provide helpful information for future work related to Ub-mediated protein regulation in plants.

## Materials and methods

### *Plant materials*

*Arabidopsis* (ecotype Columbia) seeds were germinated and cultured with shaking in liquid Murashige and Skoog medium containing 1% sucrose and 0.5 g $l^{-1}$ MES, under a 16/8 h light/dark cycle at 22 °C. MG132 (Peptide Institute, Inc., Osaka, Japan) was added to 10-d-old cultured seedlings at a final concentration of 10 μM. After 24 h treatment, the seedlings were harvested. *Nicotiana benthamiana* was grown in a temperature-controlled growth room maintained at 25 °C under a 16/8 h light/dark cycle. Four- to five-week-old plants were used for experiments.

### *Large-scale purification of Ub-related proteins*

To prepare an immunoaffinity column, HiTrap NHS-activated HP (1 ml, GE Healthcare Amersham Biosciences KK, Tokyo, Japan) was coupled with 1 mg of anti-Ub antibody FK2 (Nippon Bio-Test Laboratories, Tokyo, Japan) or mouse serum (Chemicon International, Inc., California, USA) as a negative control according to the manufacturer's instructions.

To purify Ub-related proteins under native condition, *Arabidopsis* seedlings were ground in liquid $N_2$ with a mortar and pestle, and the powder was further ground in buffer A [50 mM TRIS-HCl (pH 7.5), 150 mM NaCl] containing the Complete Protease Inhibitor cocktail (Roche Applied Science, GmbH, Mannheim, Germany), 5 mM 2-mercaptoethanol, and 10 μM MG132. The homogenate was centrifuged at 32 300 *g* for 15 min and the supernatant was centrifuged again for 5 min. The supernatant was filtered through a 0.8 μm syringe filter. The total protein extract (200–250 mg) was applied to an immunoaffinity column equilibrated with buffer A. After washing the column with 5 vols of buffer A, bound proteins were eluted with buffer B [0.1 M glycine-HCl (pH 3.0), 150 mM NaCl]. Purification of the Ub-related proteins was performed three times.

### *In-gel digestion of purified proteins, MS/MS analysis, and data reduction*

The eluted proteins from three independent purifications were mixed and fractionated by SDS-PAGE. Protein bands were detected with Flamingo™ Fluorescent Gel Stain (Bio-Rad Laboratories, CA, USA). The protein bands were excised and other smearing regions were cut into 2-mm-long gel pieces for in-gel trypsin digestion. In-gel digestion and MS/MS analysis were performed according to the methods described by Fujiwara *et al.* (2006) and Nakashima *et al.* (2008). The gel pieces were dehydrated by washing twice with 100% acetonitrile, and dried with a vacuum concentrator. The proteins were reduced with 10 mM DTT at 56 °C for 45 min and then alkylated with 55 mM iodoacetamide at room temperature in the dark for 30 min. After washing twice with 25 mM ammonium bicarbonate, the samples were dehydrated again with 50% acetonitrile and dried. The protein samples were digested with 10 μg $ml^{-1}$ proteomics-grade trypsin (Promega, Madison, WI, USA) for 12 h at 37 °C.

The digested peptides were subjected to column chromatography (PEPMAPC18, 5 μm, 75 μm internal diameter, 15 cm; Dionex, Sunnyvale, CA) using the CapLC system (Waters, Milford, MA, USA). Buffers were 0.1% formic acid in water (A) and 0.1% formic acid in acetonitrile (B). A linear gradient from 5% to 45% B for 25 min was applied, and peptides eluted from the column were introduced directly into a Q-TOF Ultima mass spectrometer (Waters) at a flow rate of 100 nl $min^{-1}$. In the ESI-positive ion mode, ionization was performed at a capillary voltage of 2.2 kV with the PicoTip nanospray source (New Objective, Cambridge, MA). For survey scan, mass spectra were acquired for the two most intense ions from the precursor ion scan between m/z 400 and 1500. For collision-induced dissociation (CID), the collision energy was set automatically according to the mass and charge state of the precursor peptide. MS/MS spectra were analysed with the MASCOT server against a protein database from the

National Center for Biotechnology Information. The applied MASCOT search parameters were as follows: (i) taxonomy: *Arabidopsis thaliana*; (ii) potential modifications: carbamidomethyl and oxidation as fixed modifications, myristoylation (N-term G, K); (iii) max missed cleavage: 1; (iv) peptide tolerance: ±0.5 Da; (v) MS/MS tolerance: ±0.2 Da; and (vi) peptide charge: $2^+$ and $3^+$. Proteins detected from peptide fragments with high reliability [MASCOT score >40 ($P$ <0.05)] were selected as identified proteins.

The presence of putative motifs in the identified proteins was analysed using Eukaryotic Linear Motif resource (ELM; http://elm.eu.org/) for destruction-box (D-box) and KEN-box, and GENETYX-MAC software for PEST sequences.

### *Antibody production*

To produce a polyclonal fructose biphosphate aldolase-like (FBA) antibody, the open reading frame (ORF) of *Arabidopsis* FBA (At3g52930) was amplified with primers 'fructose AntiB-F' (5′-GGAATTCCATATGTCTGCCTTCACAAGCAA-3′) and 'fructose AntiB-R' (5′-CGGAATTCTCAGTACTTGTAATCCTTCACG-3′), thereby introducing a *Nde*I site at the 5′ terminus and an *Eco*RI site at the 3′ terminus. The *Nde*I–*Eco*RI fragment of FBA was cloned into the expression vector pET28c (+) carrying 6×-histidine at the N terminus. The resulting plasmid was transformed into BL21 (DE3) cells. The purified histidine-tagged FBA protein was injected into a rabbit as the antigen. The antiserum obtained was used as anti-FBA antibody for immunoblot analysis.

### *Agroinfiltration*

The ORFs of At1g12840 (de-etiolated 3; DET3) and At3g04120 (glyceraldehyde-3-phosphate dehydrogenase C subunit; GAPC) were amplified from RIKEN *Arabidopsis* Full-Length cDNAs (RAFL) using the following primers: 'attB1-At1g12840-5′' (5′-GGGGACAAGTTTGTACAAAAAAGCAGGCTTCATGACTTCGAGATAT-3′) and 'attB2-At1g12840-3′' (5′-GGGGACCACTTTGTACAAGAAAGCTGGGTCAGCAAGGTTGATAGT-3′), and 'attB1-At3g04120-5′' (5′-GGGGACAAGTTTGTACAAAAAAGCAGGCTTCATGGCTGACAAGAAG-3′) and 'attB2-At3g04120-3′' (5′-GGGGACCACTTTGTACAAGAAAGCTGGGTCGGCCTTTGACATGTG-3′), respectively. Transfer of the PCR products to the entry vector pDONR221 was performed by BP reaction (Gateway; Invitrogen). Each ORF fragment of At1g12840 and At3g04120 on pDONR221 was transferred to the binary vector pGWB14 (Nakagawa *et al.*, 2007) carrying 3× HA by LR reaction (Gateway; Invitrogen).

The resulting constructs (DET3-HA and GAPC -HA) were introduced into *Agrobacterium tumefaciens* strain GV3101 by electroporation. Agroinfiltration using *N. benthamiana* leaves was performed as described previously (Katou *et al.*, 2005). Discs were collected from leaves infiltrated with *Agrobacterium* cells after infiltration for 2 d.

### *Degradation assays*

For the degradation assays of DET3-HA and GAPC-HA proteins, total protein was extracted from agro-infiltrated *N. benthamiana* leaf discs with extraction buffer C (50 mM TRIS-HCl, 2 mM ATP, 5 mM $MgCl_2$, 10 mM 2-mercaptoethanol, and 20% glycerol) supplemented with 30 μM MG132 or DMSO. For the FBA degradation assay, total protein from *Arabidopsis* seedlings was extracted with buffer C supplemented with 10 μM leupeptin (Peptide Institute) and 30 μM MG132 or DMSO. The protein extracts were incubated at room temperature for 2 h. 3× SDS sample buffer was added to stop the reaction, and the sample was used for immunoblot analysis. Anti-HA antibody was purchased from Abcam plc (Cambridge, UK). The degradation assay for each protein was replicated three times. Signal intensities of proteins detected on immunoblotted membranes were quantitated by digitizing with Image J software (http://rsbweb.nih.gov/ij/). Each quantitated value of HA or FBA signal was divided by the corresponding quantitated value of the control protein. The relative amounts of the remaining proteins (%) after incubation with MG132 or DMSO were calculated.

## Results and discussion

### *Purification and identification of Ub-related proteins from* Arabidopsis *seedlings*

To isolate Ub-related proteins by immunoaffinity chromatography, monoclonal antibody FK2 was applied, which selectively recognizes the Ub moiety but not free Ub (Fujimuro *et al.*, 1994). Approximately 250 mg of total protein was obtained from 50 g of *Arabidopsis* seedlings and applied to the immunoaffinity column under native condition (Fig. 1A). The staining pattern of eluted proteins subjected to SDS–PAGE was reproducible among the samples derived from three independent purification steps (see Supplementary Fig. S1 at *JXB* online). Compared to the mouse serum column, a number of discrete bands on a smeared background were detected in the purified sample eluted with the FK2 column (Fig. 1B), suggesting different mobilities in a gel caused by the heterogeneity of multi-Ub chains, as observed in a study of human cells (Matsumoto *et al.*, 2005).

Numerous Ubs were detected by MS/MS analysis, indicating that they were probably derived from Ub-conjugated proteins. Ubs and E2 proteins were eliminated from the list of proteins isolated with the FK2 column and the proteins isolated with the mouse serum column were further subtracted. In this study, only proteins with a score of over 40 ($P$ <0.05) were selected as candidate proteins with high reliability. Accordingly, 196 proteins, which were represented by 251 distinct genes including possible paralogs, were determined as Ub-related proteins (see Supplementary Table S1 at *JXB* online). Comparing the

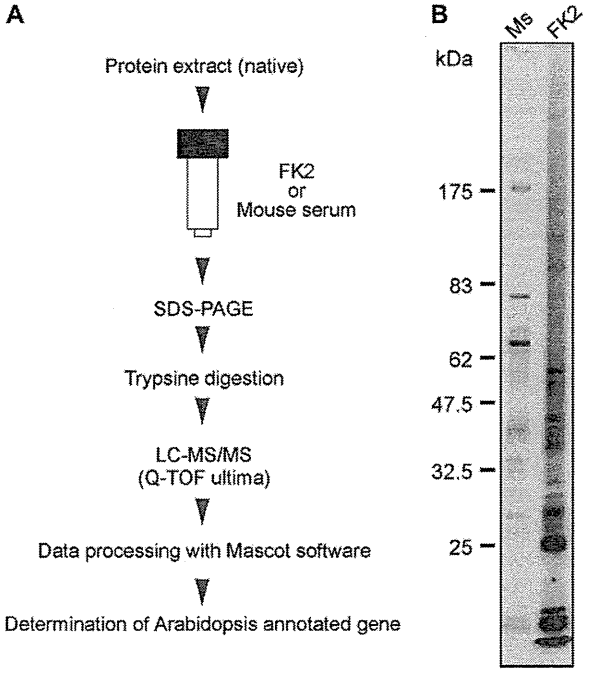


**Fig. 1.** Immunoaffinity purification and identification of Ub-related proteins. (A) Flow chart of purification and identification of Ub-related proteins. (B) Immunopurified proteins with FK2 or mouse serum (Ms) from *Arabidopsis* seedlings were subjected to SDS-PAGE and stained with Flamingo™.

results of this study with *Arabidopsis* ubiquitinated proteomes reported in two studies, 33 proteins were overlapped and only one protein (β-tubulin; protein no. 137 in Supplementary Table S1 at *JXB* online) was common to the three studies (see Supplementary Table S1 at *JXB* online). The low overlapping result compared to the previous studies may be due to the difference in the differentiation state of the protein source. In addition, unstructured threshold settings for protein screening from the MS scores may account for the difference in listed proteins among the three studies. The following reasons are proposed. Immunopurification with FK2 used in this study, enabled recognition of all types of ubiquitinated proteins, whereas each UBA used in the other studies had distinct specificity to ubiquitinated proteins. Therefore, the dominant ubiquitinated proteins were preferentially trapped by FK2. In addition, our dataset included a high proportion of associated proteins of ubiquitinated proteins due to the native condition used in protein purification. In fact, proteins annotated as RING-type E3 (protein no. 109 in Supplementary Table S1 at *JXB* online) and putative Ub receptors, DNA-repair protein RAD23 (protein no. 119 in Supplementary Table S1 at *JXB* online), and UBA-like motif-containing protein (protein no. 196 in Supplementary Table S1 at *JXB* online), were identified in this study, suggesting that non-direct target proteins for ubiquitination were also isolated.

### *Characterization of Ub-related proteins from* Arabidopsis *seedlings*

The identified proteins were categorized on the basis of the biological processes described in 'The *Arabidopsis* Information Resource' (TAIR) (Fig. 2A). The large population of proteins involved in metabolism (23.0%) as well as previous *Arabidopsis* ubiquitinated proteomes (Maor *et al.*, 2007; Manzano *et al.*, 2008) may indicate the significance of ubiquitination for protein regulation in cellular metabolism. Similar to the previous report of Manzano *et al.* (2008), it was found that the proteins involved in stress response (21.4%) were more abundant in seedlings than in cell cultures. This might be due to the differentiation state of the cells, because the growth condition in liquid culture seemed to be more stressful for seedlings than for cell cultures. Indeed, proteins involved in abiotic stress were dominant in this category (Fig. 2A). The majority of translational proteins identified in our study (16.8%) were ribosomes, in agreement with Maor's study (Maor *et al.*, 2007). It has been speculated that ubiquitination might play an important role in the regulation and/or quality control of ribosomal proteins, as reported in human cells (Matsumoto *et al.*, 2005). In addition, the recent report by Kraft *et al.* (2008) of a link between ubiquitination and regulated degradation of mature ribosomes in yeast also supports our results. The percentage of proteins involved in signal transduction (1.5%) was lower than that previously reported for the ubiquitinated proteome from *Arabidopsis* seedlings (Manzano *et al.*, 2008). The difference may depend on the threshold for the screening of identified proteins from MS scores, as described above. Only proteins with a high reliability (95% confidence) were listed in this study, whereas Manzano's list contained proteins with low reliability (Manzano *et al.*, 2008). The proportions of other components were similar to that found in previous *Arabidopsis* ubiquitinated proteomes. One significant difference compared to the previous *Arabidopsis* ubiquitinated proteomes was the high percentage of proteasome subunits (14.3%), which was probably dependent on the native condition for protein purification. This fact indicated that the associated proteins of ubiquitinated proteins were isolated as well, and implied that most proteins were involved in Ub/proteasome-dependent proteolysis.

### *Classification of identified proteins*

Purification under native condition is a feasible technique to identify Ub-related proteins that play major roles in Ub-dependent regulation (Matsumoto *et al.*, 2005). Since the protein population isolated under native condition included not only ubiquitinated proteins but also their associated proteins, they were classified as ubiquitinated proteins and their associated proteins based on the following three criteria.

First, previous *Arabidopsis* ubiquitinated proteomes from cell cultures and seedlings, respectively, were examined (Maor *et al.*, 2007; Manzano *et al.*, 2008). Of the proteins identified in our study, 33 have been reported as

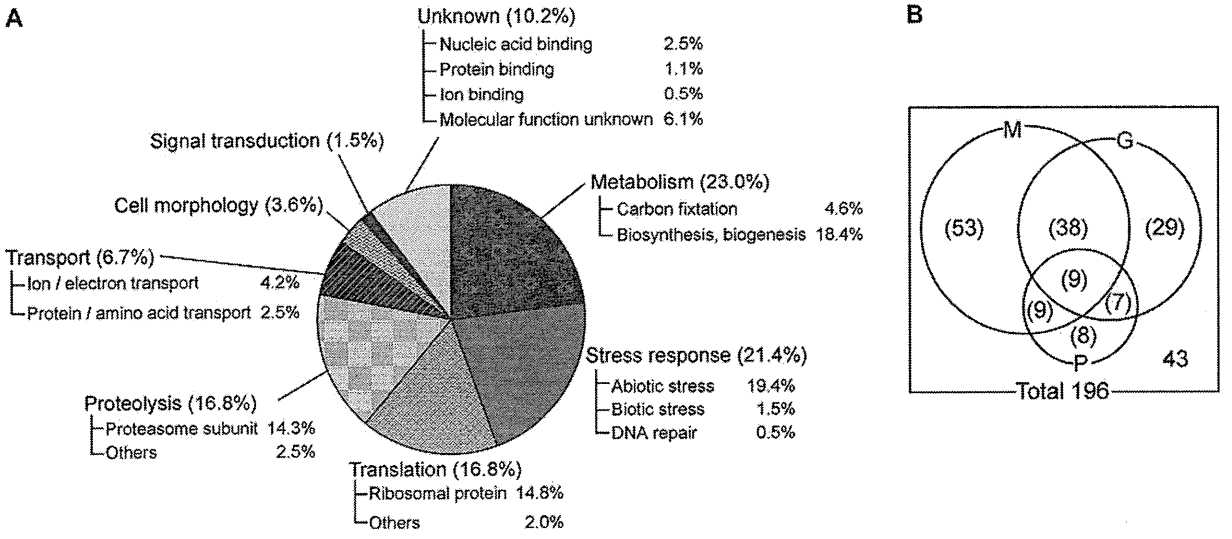


**Fig. 2.** Characterization of proteins identified from *Arabidopsis* seedlings. (A) Proportion of identified proteins categorized according to function. Each category was further subdivided according to specific function. (B) Numbers of potential ubiquitinated proteins and their associated proteins. Number outside the circles indicates the number of associated proteins of ubiquitinated proteins. M, proteins containing at least one motif; G, proteins detected in multiple gel pieces; P, proteins previously reported as ubiquitinated proteins.

ubiquitinated proteins, suggesting that these were the potential direct targets of ubiquitination (Fig. 2B; see Supplementary Table S1 at *JXB* online).

Second, the identified proteins were classified on the basis of potential ubiquitination-targeting signal motifs (D-box, KEN-box, and PEST sequence) to predict the ubiquitinated proteins. D-box and KEN-box are short sequence elements in the substrates of the anaphase-promoting complex/cyclosome (APC/C), which is a multisubunit RING-type E3 (King *et al.*, 1996; Pfleger and Kirschner, 2000), and indeed, RING-type E3 (protein no. 109 in Supplementary Table S1 at *JXB* online) was found in our study. PEST sequences that are rich in proline (P), glutamic acid (E), serine (S), and threonine (T) were found in a number of short-lived proteins controlled by proteolysis, mostly via ubiquitin-mediated degradation. Almost half of the identified proteins (109/196 proteins (55.6%)) contained at least one motif, implying that they are the potential targets of Ub/proteasome-dependent proteolysis (Fig. 2B; see Supplementary Tables S1 and S2 at *JXB* online).

Third, multiple detections from different gel pieces implied multi-ubiquitination of the proteins, since the heterogeneity of multi-Ub chains accounted for the different mobilities in a gel. Of the identified 196 Ub-related proteins, 83 (42.3%) were found in 2–17 gel pieces of different sizes (Fig. 2B; see Supplementary Table S1 at *JXB* online), suggesting that the proteins were probably tagged with heterogeneous multi-Ub chains.

Considering potential ubiquitination-targeting signal motifs, in-gel mobilities of the identified proteins, and previous reports, 153 proteins (78.0%) were predicted as the potential targets of ubiquitination, including 109 potential target proteins (55.6%) of Ub/proteasome-dependent proteolysis, whereas the remaining proteins (21.9%) were potential molecules associated with the ubiquitinated proteins.

### *Degradation assays of proteins predicted as ubiquitinated proteins*

The results suggested that a large proportion of the identified proteins were involved in Ub/proteasome-dependent proteolysis. Therefore, the identified proteins were examined by proteasome degradation assay. According to the prediction described above, three proteins predicted as potential ubiquitinated proteins, At1g12840 (DET3, protein no. 82 in Supplementary Table S1 at *JXB* online), At3g04120 (GAPC, protein no. 1 in Supplementary Table S1 at *JXB* online), and At3g52930 (fructose biphosphate aldolase-like; FBA, protein no. 6 in Supplementary Table S1 at *JXB* online), were chosen for the assay.

DET3 encodes subunit C of vacuolar $H^+$-ATPase (V-ATPase). V-ATPase is one of the major proton pumps that act to acidify intracellular compartments (Sze *et al.*, 2002) and DET3 is significantly responsible for its activity (Schumacher *et al.*, 1999). Since DET3 contains four D-box motifs and was detected in two gel pieces (Supplementary Table S1 at *JXB* online), regulation of DET3 protein by Ub/proteasome-dependent proteolysis was highly expected. DET3 protein tagged with 3× HA was transiently expressed in *N. benthamiana* leaves by agroinfiltration. The protein extract was incubated with MG132, a 26S proteasome inhibitor. As a result, it was found that DET3 protein degradation was inhibited by MG132 treatment but not DMSO treatment (Fig. 3A), indicating that it was conjugated with canonical Ub chains and then underwent the

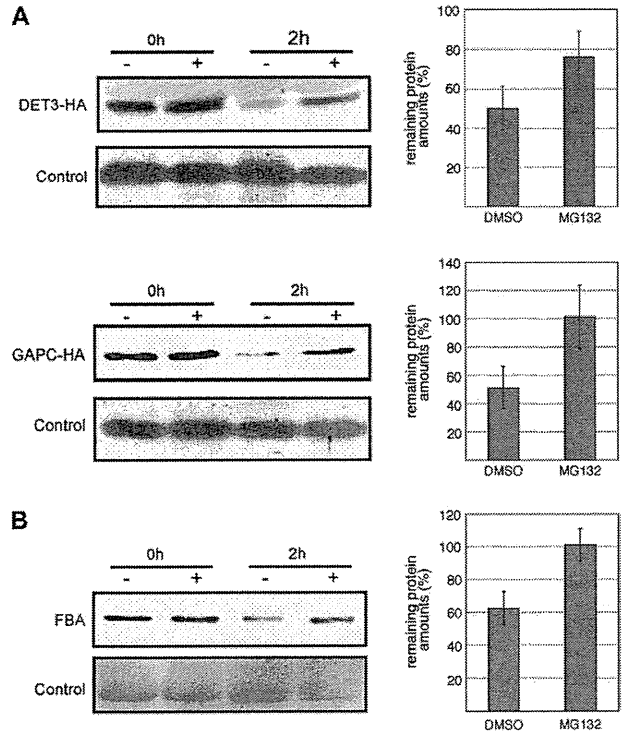


**Fig. 3.** Degradation assays of potential ubiquitinated proteins. Protein extracts were treated with MG132 (+) or DMSO (–). Lower panels of each figure indicate loading controls. Graphs on the right represent the relative amount of remaining protein (%) after treatment with MG132 (+) or DMSO. Error bars indicate standard deviations. (A) DET3-HA and GAPC-HA proteins transiently expressed in *N. benthamiana* leaves were detected with anti-HA antibody. (B) Total proteins were extracted from *Arabidopsis* seedlings. Immunoblot analysis was performed with anti-FBA antibody.

proteasome-dependent proteolysis. Other subunits A and B of V-ATPase were respectively isolated as ubiquitinated proteins in Maor's and Manzano's studies (Maor *et al.*, 2007; Manzano *et al.*, 2008), whereas the anti-Ub antibody used in our study could trap all of these subunits, implying that the difference in the identified subunits of V-ATPase may be attributed to the distinct specificity of the ligands used for affinity purification. It was also suggested that each subunit is ubiquitinated by a distinct ubiquitination pathway, and at least one subunit DET3 of the V-ATPase complex was degraded by the 26S proteasome.

GAPC was detected in four gel pieces, although the ubiquitination-targeting signal motif was absent (see Supplementary Table S1 at *JXB* online). The degradation of GAPC by the 26S proteasome has not been reported to date. Since it has also been reported as a ubiquitinated protein (Manzano *et al.*, 2008), the degradation by the 26S proteasome of the GAPC protein, which was transiently expressed similar to DET3, was examined. As shown in Fig. 3A, the degradation of the GAPC protein was inhibited by MG132 treatment, but not DMSO treatment, indicating that it was regulated by the Ub/proteasome-dependent proteolysis.

FBA was identified in seven gel pieces, although it did not contain any potential ubiquitination-targeting signal motifs (see Supplementary Table S1 at *JXB* online). FBA was also identified as a ubiquitinated protein (Maor *et al.*, 2007). Thus, it was expected that FBA would be degraded by the 26S proteasome. To examine the FBA degradation by the 26S proteasome in *Arabidopsis* seedlings, the protein extract was incubated with or without MG132, and FBA protein was detected with its antibody. As shown in Fig. 3B, the degradation of FBA was inhibited by MG132, demonstrating that FBA was regulated by Ub/proteasome-dependent proteolysis in *Arabidopsis* seedlings.

The degradation of DET3, GAPC, and FBA by the 26S proteasome was demonstrated for the first time in this study. GAPC and FBA are involved in glycolysis and are known to respond to environmental stress. Thus, the turnover of these proteins may be regulated by the Ub/proteasome-dependent proteolysis in the glycolytic pathway and/or stress response. It would be interesting to investigate the contribution of Ub-mediated regulation of these proteins in metabolism and/or stress response as a future work.

## Conclusions

This study showed the Ub-related proteome of *Arabidopsis* seedlings. Protein purification under native conditions with an anti-Ub antibody contributed to the isolation of various Ub-related proteins that mainly comprised proteins involved in Ub/proteasome-dependent proteolysis. The protein population identified contained both the targets of ubiquitination and their associated proteins. Biochemical evidence is required to characterize exactly which protein is the direct target of ubiquitination. Nevertheless, classification of the identified proteins based on the potential ubiquitination-targeting signal motifs, in-gel mobilities, and the previous reports contributed to the prediction of ubiquitinated proteins and their associated proteins. Our results are expected to be of use to the future investigation of Ub-mediated protein regulation in plants.

## Supplementary data

Supplementary data are available at *JXB* online.

**Supplementary Fig. S1.** Respective SDS-PAGE images of proteins immunopurified with FK2 obtained from three independent experiments (Ex1, Ex2, and Ex3). The staining pattern of the purified proteins was reproducible.

**Supplementary Table S1.** Ub-related proteins identified from *Arabidopsis* seedlings.

**Supplementary Table S2.** Proteins containing potential ubiquitination-targeting signal motifs for Ub/proteasome-dependent proteolysis.

## Acknowledgements

We thank Dr T Nakagawa (Shimane University, Japan) for pGWB14 vector and Ms R Okanami for technical assistance. This work was supported by KAKENHI (19658041), a Grant-in-Aid for Exploratory Research from the Japan Society for the Promotion of Science (JSPS), and a Grant-in-Aid for Scientific Research from the Nara Institute of Science and Technology supported by the Ministry of Education, Culture, Sports, Science, and Technology, Japan.

## References

**Bachmair A, Novatchkova M, Potuschak T, Eisenhaber F.** 2001. Ubiquitylation in plants: a post-genomic look at a post-translational modification. *Trends in Plant Science* **6,** 463–470.

**Fujimuro M, Sawada H, Yokosawa H.** 1994. Production and characterization of monoclonal antibodies specific to multi-ubiquitin chains of polyubiquitinated proteins. *FEBS Letters* **349,** 173–180.

**Fujiwara M, Umemura K, Kawasaki T, Shimamoto K.** 2006. Proteomics of Rac GTPase signaling reveals its predominant role in elicitor-induced defense response of cultured rice cells. *Plant Physiology* **140,** 734–745.

**Haglund K, Dikic I.** 2005. Ubiquitylation and cell signaling. *EMBO Journal* **24,** 3353–3359.

**Hatfield PM, Gosink MM, Carpenter TB, Vierstra RD.** 1997. The ubiquitin-activating enzyme (E1) gene family in *Arabidopsis thaliana*. *The Plant Journal* **11,** 213–226.

**Hatakeyama S, Matsumoto M, Nakayama KI.** 2005. Mapping of ubiquitination sites on target proteins. *Methods in Enzymology* **399,** 277–286.

**Hershko A, Ciechanover A.** 1998. The ubiquitin system. *Annual Review of Biochemistry* **67,** 425–479.

**Jeon HB, Choi ES, Yoon JH, Hwang JH, Chang JW, Lee EK, Choi HW, Park ZY, Yoo YJ.** 2007. A proteomics approach to identify the ubiquitinated proteins in mouse heart. *Biochemical and Biophysical Research Communications* **357,** 731–736.

**Katou S, Karita E, Yamakawa H, Seo S, Mitsuhara I, Kuchitsu K, Ohashi Y.** 2005. Catalytic activation of the plant MAPK phosphatase NtMKP1 by its physiological substrate salicylic acid-induced protein kinase but not by calmodulins. *Journal of Biological Chemistry* **280,** 39569–39581.

**King RW, Glotzer M, Kirschner MW.** 1996. Mutagenic analysis of the destruction signal of mitotic cyclins and structural characterization of ubiquitinated intermediates. *Molecular Biology of the Cell* **7,** 1343–1357.

**Kraft C, Deplazes A, Sohrmann M, Peter M.** 2008. Mature ribosomes are selectively degraded upon starvation by an autophagy pathway requiring the Ubp3p/Bre5p ubiquitin protease. *Nature Cell Biology* **10,** 602–610.

**Kraft E, Stone SL, Ma L, Su N, Gao Y, Lau OS, Deng XW, Callis J.** 2005. Genome analysis and functional characterization of the E2 and RING-type E3 ligase ubiquitination enzymes of Arabidopsis. *Plant Physiology* **139,** 1597–1611.

**Manzano C, Abraham Z, López-Torrejón G, Del Pozo JC.** 2008. Identification of ubiquitinated proteins in Arabidopsis. *Plant Molecular Biology* **68,** 145–158.

**Maor R, Jones A, Nühse TS, Studholme DJ, Peck SC, Shirasu K.** 2007. Multidimensional protein identification technology (MudPIT) analysis of ubiquitinated proteins in plants. *Molecular and Cellular Proteomics* **6,** 601–610.

**Matsumoto M, Hatakeyama S, Oyamada K, Oda Y, Nishimura T, Nakayama KI.** 2005. Large-scale analysis of the human ubiquitin-related proteome. *Proteomics* **5,** 4145–4151.

**Mazzucotelli E, Belloni S, Marone D, De Leonardis AM, Guerra D, Di Fonzo N, Cattivelli L, Mastrangelo AM.** 2006. The e3 ubiquitin ligase gene family in plants: regulation by degradation. *Current Genomics* **7,** 509–522.

**Nakagawa T, Kurose T, Hino T, Tanaka K, Kawamukai M, Niwa Y, Toyooka K, Matsuoka K, Jinbo T, Kimura T.** 2007. Development of series of gateway binary vectors, pGWBs, for realizing efficient construction of fusion genes for plant transformation. *Journal of Bioscience and Bioengineering* **104,** 34–41.

**Nakashima A, Chen L, Thao NP, Fujiwara M, Wong HL, Kuwano M, Umemura K, Shirasu K, Kawasaki T, Shimamoto K.** 2008. RACK1 functions in rice innate immunity by interacting with the Rac1 immune complex. *The Plant Cell* **20,** 2265–2279.

**Peng J, Schwartz D, Elias JE, Thoreen CC, Cheng D, Marsischky G, Roelofs J, Finley D, Gygi SP.** 2003. A proteomics approach to understanding protein ubiquitination. *Nature Biotechnology* **21,** 921–926.

**Pfleger CM, Kirschner MW.** 2000. The KEN box: an APC recognition signal distinct from the D box targeted by Cdh1. *Genes and Development* **14,** 655–665.

**Pickart CM.** 2001. Mechanisms underlying ubiquitination. *Annual Review of Biochemistry* **70,** 503–533.

**Schumacher K, Vafeados D, McCarthy M, Sze H, Wilkins T, Chory J.** 1999. The *Arabidopsis det3* mutant reveals a central role for the vacuolar $H^+$-ATPase in plant growth and development. *Genes and Development* **13,** 3259–3270.

**Sze H, Schumacher K, Müller ML, Padmanaban S, Taiz L.** 2002. A simple nomenclature for a complex proton pump: VHA genes encode the vacuolar $H^+$-ATPase. *Trends in Plant Science* **7,** 157–161.

**Thrower JS, Hoffman L, Rechsteiner M, Pickart CM.** 2000. Recognition of the polyubiquitin proteolytic signal. *EMBO Journal* **19,** 94–102.

**Yanagawa Y, Sullivan JA, Komatsu S, *et al.*** 2004. *Arabidopsis* COP10 forms a complex with DDB1 and DET1 *in vivo* and enhances the activity of ubiquitin conjugating enzymes. *Genes and Development* **18,** 2172–2181.

BMC Plant Biology

BioMed Central

Methodology article

Open Access

# A simple and high-sensitivity method for analysis of ubiquitination and polyubiquitination based on wheat cell-free protein synthesis

Hirotaka Takahashi[1,2], Akira Nozawa[1,2,5], Motoaki Seki[3], Kazuo Shinozaki[4], Yaeta Endo*[1,2,5] and Tatsuya Sawasaki*[1,2,5]

Address: [1]Cell-Free Science and Technology Research Center, Ehime University, Matsuyama 790-8577, Japan, [2]The Venture Business laboratory, Ehime University, Matsuyama 790-8577, Japan, [3]Plant Functional Genomics Research Group, 1-7-22 Suehiro-cho, Tsurumi-ku, Yokohama, Kanagawa 230-0045, Japan, [4]Gene Discovery Research Group, RIKEN Plant Science Center, 1-7-22 Suehiro-cho, Tsurumi-ku, Yokohama, Kanagawa 230-0045, Japan and [5]RIKEN Genomic Sciences Center, 1-7-22 Suehiro-cho, Tsurumi-ku, Yokohama, Kanagawa 230-0045, Japan

Email: Hirotaka Takahashi - h-takahashi@ccr.ehime-u.ac.jp; Akira Nozawa - anozawa@ccr.ehime-u.ac.jp; Motoaki Seki - mseki@psc.riken.jp; Kazuo Shinozaki - sinozaki@rtc.riken.jp; Yaeta Endo* - yendo@eng.ehime-u.ac.jp; Tatsuya Sawasaki* - sawasaki@eng.ehime-u.ac.jp

* Corresponding authors

Published: 6 April 2009

*BMC Plant Biology* 2009, **9**:39 doi:10.1186/1471-2229-9-39

Received: 26 December 2008
Accepted: 6 April 2009

This article is available from: http://www.biomedcentral.com/1471-2229/9/39

© 2009 Takahashi et al; licensee BioMed Central Ltd.
This is an Open Access article distributed under the terms of the Creative Commons Attribution License (http://creativecommons.org/licenses/by/2.0), which permits unrestricted use, distribution, and reproduction in any medium, provided the original work is properly cited.

## Abstract

**Background:** Ubiquitination is mediated by the sequential action of at least three enzymes: the E1 (ubiquitin-activating enzyme), E2 (ubiquitin-conjugating enzyme) and E3 (ubiquitin ligase) proteins. Polyubiquitination of target proteins is also implicated in several critical cellular processes. Although Arabidopsis genome research has estimated more than 1,300 proteins involved in ubiquitination, little is known about the biochemical functions of these proteins. Here we demonstrate a novel, simple and high-sensitive method for *in vitro* analysis of ubiquitination and polyubiquitination based on wheat cell-free protein synthesis and luminescent detection.

**Results:** Using wheat cell-free synthesis, 11 E3 proteins from Arabidopsis full-length cDNA templates were produced. These proteins were analyzed either in the translation mixture or purified recombinant protein from the translation mixture. In our luminescent method using FLAG- or His-tagged and biotinylated ubiquitins, the polyubiquitin chain on AtUBC22, UPL5 and UPL7 (HECT) and CIP8 (RING) was detected. Also, binding of ubiquitin to these proteins was detected using biotinylated ubiquitin and FLAG-tagged recombinant protein. Furthermore, screening of the RING 6 subgroup demonstrated that At1g55530 was capable of polyubiquitin chain formation like CIP8. Interestingly, these ubiquitinations were carried out without the addition of exogenous E1 and/or E2 proteins, indicating that these enzymes were endogenous to the wheat cell-free system. The amount of polyubiquitinated proteins in the crude translation reaction mixture was unaffected by treatment with MG132, suggesting that our system does not contain 26S proteasome-dependent protein degradation activity.

**Conclusion:** In this study, we developed a simple wheat cell-free based luminescence method that could be a powerful tool for comprehensive ubiquitination analysis.

## Background

Protein ubiquitination plays a crucial role in numerous cellular processes such as cell growth, regulation of diverse signal transduction and disease [1-3]. The covalent attachment of ubiquitin to protein substrates requires a stepwise cascade of enzymatic reactions. First, ubiquitin is activated by E1 (ubiquitin-activating enzyme, UBA) in an ATP-dependent manner by forming a high-energy thioester-bond between the carboxyl-terminal glycine residue of ubiquitin and a cysteine residue of E1. The activated ubiquitin is then transferred to the core-cysteine residue of E2 (ubiquitin-conjugating enzyme, UBC). Together with an E3 ligase enzyme, ubiquitin is attached via its carboxyl-terminus to an e-amino group of a lysine residue in the target protein. Since E3 binds to both E2 and the target protein, and acts as scaffold between E2 and the substrate protein, the E3 ligase is the major determinant for selecting target proteins for ubiquitination. There is large number of genes encoding E3 ligases in all eukaryotes, and the diversity of E3s is thought to contribute to the substrate specificity of numerous target proteins. E3 ligases are structurally divided into three groups: HECT, RING and U-box [4]. The HECT-type E3 ligase is distinct from the other two ligases in that it forms a thioester-bond with ubiquitin prior to the transfer of ubiquitin to target proteins. The RING-type E3 ligase contains a unique domain similar to the zinc finger motif that mediates protein-protein interactions [5] and is further divided into two classes: one that can function alone and another that forms a complex with other E3 components [4].

Recent studies have shown that attachment of polyubiquitin chains on target proteins linked via lysine-48 of ubiquitin typically leads to degradation by the 26S proteasome [6], whereas linkage via lysine-63 mediates different pathways such as internalization of membrane proteins, activation of signal transduction and DNA damage repair [7]. The formation of lysyl-63-linked polyubiquitin chains is generated by specific combinations of E2s and E2 variants, which are similar to E2s except that they lack core cysteine residues required for E2 activity [8,9]. In addition, ubiquitination of substrates without polymerization, mono-ubiquitination, acts as a sorting signal for protein endocytosis and as a regulation factor for diverse proteins, including histones and transcription factors [10].

In plant, genomic research of the model plant *Arabidopsis thaliana* showed that there are two E1s, 37 E2s and more than 1,300 predicted E3s [11]. Although little is known about protein ubiquitination in plants compared with yeast and mammals, recent studies revealed that the plant ubiquitination pathway is involved in the regulation of morphogenesis, the circadian clock and responding to hormone or pathogen signal molecules [12-15]. Despite the importance of ubiquitination in plants, much of the plant ubiquitination cascade is still unknown because of its complexity and the issues inherent to the use of Arabidopsis plants for biochemical analysis. Although several interactions between E2s and RING type E3s have been demonstrated *in vitro* using recombinant proteins expressed in *Escherichia coli*, these efforts are hampered by the inability to obtain functional protein using conventional methods [16].

With this in mind, we sought to develop a novel *in vitro* method to analyze the ubiquitin pathway genome-wide. The two major obstacles hindering the development of an *in vitro* assay for genome-wide screening are the difficulty of efficiently producing recombinant protein and the inability to detect ubiquitination in a high-throughput fashion. To address the first problem we used the wheat cell-free protein synthesis system, which has been previously reported to produce a wide range of functional Arabidopsis and human proteins [17-19]. Moreover, a collection of RIKEN Arabidopsis Full Length (RAFL) cDNA clones covering about 70% of Arabidopsis genes is available [20]. Using these RAFL clones as templates, recombinant proteins involved in the ubiquitination pathway were expressed in the wheat cell-free system and used for several functional analyses. For screening, conventional detection methods such as immunoblot analysis or radioisotope-labeled proteins are not suitable for the detection of a large number of ubiquitination reactions. Recently, a high-throughput luminescence method to detect protein ubiquitination was reported [21], however this method requires purified protein and creation of specialized vectors to produce proteins. In this study, a novel *in vitro* assay to detect polyubiquitin chain formation was developed using wheat cell-free synthesis and a modified luminescence-based detection method. We demonstrate (1) creation of a simple *in vitro* method to detect polyubiquitination using crude recombinant E3s, (2) discovery of the activity of At1g55530 by screening a RING subgroup in the reported assay, and (3) the polyubiquitination assay in the presence of MG132 demonstrated the absence of 26S proteasome-dependent protein degradation activity in wheat cell-free system.

## Results

### *Detection of Polyubiquitin Chains on AtUBC22 E2 enzyme*

Recently, AtUBC22 (At5g05080) E2 protein has been shown to catalyze polyubiquitin chain formation without an E3 ligase, although AtUBC35 (At1g78870) E3-independent polyubiquitination activity could not be detected [16]. We employed AtUBC22 and AtUBC35 as model E2 proteins to develop a novel polyubiquitination assay. We have also demonstrated that addition of biotin ligase (BirA) and biotin to the wheat cell-free protein production system yields a single biotinylation on a target pro-

tein containing a biotin ligation site [22]. Using this method, biotinylated recombinant AtUBC22 and AtUBC35 were synthesized and, without purification from the translation mixture, the polyubiquitination reaction was performed on the crude recombinant protein. After the reaction, biotinylated AtUBC22 and AtUBC35 were purified using streptavidin-conjugated magnetic beads and the polyubiquitin chain was detected by immunoblot analysis. As shown in Fig 1A, AtUBC22 showed polyubiquitination, whereas AtUBC35 showed mainly monoubiquitination. Interestingly, both E2s still had activity in absence of exogenous E1 in polyubiquitin reaction mixture (Fig. 1A, middle lanes), suggesting that wheat cell-free system has high endogenous E1 activity.

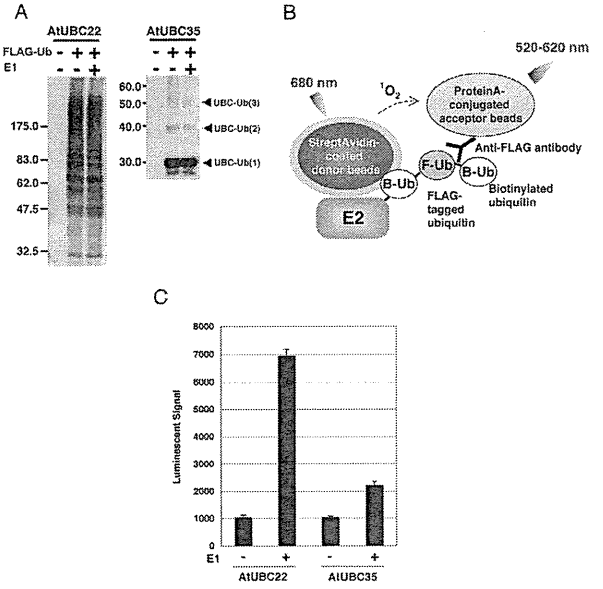


**Figure 1**
**Detection of E3-independent polyubiquitination of AtUBC22 by luminescent analysis.** A, Polyubiquitin chain on AtUBC22 but not on AtUBC35 was detected by immunoblot analysis. In this assay, polyubiquitination reaction was carried out with FLAG-tagged ubiquitin, and detected by immunoblot analysis using anti-FLAG antibody. B, Schematic diagram of detection of polyubiquitin chains by luminescent analysis. Protein A-conjugated acceptor beads and streptavidin-coated donor beads are bound to anti-FLAG antibody bound to FLAG-tagged ubiquitin and biotinylated E2, respectively, and these two beads are in closed proximity when polyubiquitin chain formed. Upon excitation 680 nm, a singlet oxygen is generated from the donor beads, and then transferred to the acceptor beads within 200 nm, and the singlet oxygen reacts the acceptor beads which in turn emits light at 520–620 nm. This light is measured by AlphaScreen kit and change to signal value. C, Polyubiquitin chain on purified recombinant E2 was detected by luminescent analysis in the presence (E1 +) or absence (E1 -) of exogenous E1. Error bars represent standard deviations from three independent experiments.

While immunoblot analysis is an excellent detection method, it is not suitable for high-throughput detection of numerous polyubiquitination reactions. Initially, we attempted to use luminescent analysis, based on the AlphaScreen technology, to detect the polyubiquitination activity of AtUBC22 and AtUBC35. In principle, if a polyubiquitin chain is formed by FLAG-tagged and biotinylated ubiquitins, it will bring into proximity the streptavidin-coated donor bead (bound to biotin) and the protein A-conjugated acceptor bead (bound to anti-FLAG IgG), producing a luminescent signal (Fig. 1B). Considering that the wheat cell-free system has high endogenous E1 activity (Fig. 1A), it may also have endogenous E2 and E3 activity. In order to avoid formation of polyubiquitin chains by an endogenous wheat germ ubiquitin pathway, purified E2s were used in this assay. As shown in Fig 1C, high luminescent signal was observed in the presence of AtUBC22 in E1-dependent manner. In contrast, AtUBC35 showed low signal. The two luminescent signals were approximately consistent with immunoblot data that AtUBC22 and AtUBC35 have high and low polyubiquitination activities respectively, as demonstrated in Fig 1A. These results indicate that the luminescent method can detect polyubiquitin chain formation by using the two types of ubiquitins.

### *Ubiquitination and Polyubiquitination Analyses of HECT-TypeE3 Ligases*

Polyubiquitination activity of E3 ligases activated by the step-wise E1 to E3 cascade is well documented [3]. We next attempted to reconstruct this cascade *in vitro* and to detect the E3-formed polyubiquitin chains using our luminescent method. Due to the size of HECT-type E3 ligases, ranging from 100 to 428 kDa in Arabidopsis, production of active protein by traditional expression methods may not be easy and biochemical analysis using only truncated recombinant protein has been carried out previously [23]. We attempted to produce full-length Arabidopsis HECT-type E3 ligase proteins using the wheat cell-free system and monitored ubiquitin-conjugation and polyubiquitination by luminescence. Two genes that encode Arabidopsis HECT-type E3 ligase, *UPL5* and *UPL7* [24], were analyzed in this study. We obtained UPL5 and UPL7 cDNA from the RAFL library and produced FLAG-tagged protein in the wheat cell-free system. Ubiquitination of FLAG-labeled UPLs (UPL-FLAGs) was investigated by both the luminescent and immunoblot methods. The successful production of the two recombinant HECT proteins was observed by immunoblot analysis (Fig. 2A) and used in the luminescence assay without purification. To detect ubiquitination of the HECT proteins, UPL-FLAGs